Model-driven mitigation measures for reopening schools during the COVID-19 pandemic.

Ryan S. McGee[*,1,a], Julian R. Homburger[*,2,b], Hannah E. Williams[2,c], Carl T. Bergstrom[†,1,d], and Alicia Y. Zhou[†,2,e]

[*]Co-first authors; corresponding authors. [†]Co-senior authors.

[1]Department of Biology, University of Washington, Seattle WA 98195

[2]Color Health, Burlingame, CA

Email: [a]ryansmcgee@gmail.com, [b]jrh@color.com, [c]hannah@color.com, [d]cbergst@uw.edu, [e]alicia@color.com

Abstract: Reopening schools is an urgent priority as the COVID-19 pandemic drags on throughout much of the world. To explore the risks associated with returning to in-person learning and the value of mitigation measures in a school setting, we use the stochastic, network-based SEIRS+ epidemiological modeling platform to simulate SARS-CoV-2 transmission in schools. Because children and adolescents differ both in disease susceptibility and in patterns of social interaction, we use distinct models of SARS-CoV-2 transmission for primary and secondary school settings. We find that a number of mitigation measures may prove useful, particularly when community prevalence is low. Student cohorting, in which students are divided into two separate populations that attend in-person classes on alternating schedules, can reduce both the likelihood and the size of outbreaks. Proactive testing of teachers and staff once or twice a week can help catch introductions early, before they spread widely through the school. Especially in secondary schools, once- or twice- weekly testing amongst students should also be considered to further reduce the likelihood of a large outbreak amongst the full population. Vaccinating teachers and staff protects these individuals and may also have a disproportionate protective effect on the outbreak potential in primary and secondary schools when vaccines block SARS-CoV-2 transmission in addition to symptoms. Other mitigation strategies – including mask-wearing, social distancing, and increased ventilation – remain a crucial component of any reopening plan.

Introduction

As the COVID-19 pandemic accelerated in early 2020, schools across the world closed preemptively in an effort to reduce transmission and protect their students, teachers, and staff. By mid-April of that year, 195 countries had closed their schools in response to COVID-19, affecting more than 1.5 billion students (1). In the United States (US), schools were among the first organizations to close, and many remained closed through the end of the 2019-20 school year or transitioned to remote learning.

While remote learning affords students the opportunity to continue their education, it fails to provide many of the crucial benefits students typically receive through in-person schooling. A recent report from the Organisation for Economic Co-operation and Development estimates that learning losses from school closures could have lasting impacts for students, equating to a 3% lower income over their lifetime (2). The United Nations Children's Fund (UNICEF) recently issued a comprehensive six-point plan for keeping schools open, which stressed the need to take immediate action to safeguard the future health and well-being of millions of children (3), and the Rockefeller Foundation issued an ambitious report advocating aggressive testing as a step toward reopening all US schools by Spring 2021 (4). Professional societies, including the National Academies of Sciences, Engineering, and Medicine and the American Academy of Pediatrics, have strongly advocated for the return to in-person learning, while also stressing the importance of using a multi-layer approach to protect students, teachers, and staff from COVID-19 risk (5, 6).

To date, limited data about COVID-19 in schools and conflicting public health guidance have made reopening schools a difficult undertaking. Furthermore, widespread community transmission and the emergence of new SARS-CoV-2 variants associated with higher transmissibility have compounded the challenges schools face when reopening (7–9). Numerous epidemiological models have been developed to estimate the spread of SARS-CoV-2 or compare the effectiveness of mitigation strategies in communities or large populations (10–16). However, only a few models have focused on estimating the spread of outbreaks and the use of different mitigation strategies specifically within the unique demographic and contact structures of primary and secondary school settings (17, 18). There is an urgent need to evaluate the effectiveness of evidence-based strategies that would allow children, teachers, and staff to return to in-person learning.

To better understand the risks associated with reopening schools and returning to in-person learning, we developed an epidemiological model to simulate the spread of SARS-CoV-2 amongst students, teachers, and staff in primary and secondary schools. Here, we use the model to explore the effectiveness of different mitigation strategies, including student cohorting, quarantine protocols, proactive testing, and vaccination. Because novel, more transmissible strains have recently emerged, we further use the model to understand how school reopening may be impacted under

conditions where these new strains become predominant.

Model and methods

A stochastic network-based model of COVID-19 transmission

We use the SEIRS+ modeling framework (https://github.com/ryansmcgee/seirsplus) to study the dynamics of disease transmission associated with school populations. SEIRS+ builds upon classic SEIR compartment models that divide the population into susceptible (S), exposed (E), infectious (I), and recovered (R) individuals (19). Over time, individuals transition between these states at rates determined by the disease characteristics. SEIR models are expressed as deterministic mass action differential equations that implicitly assume homogeneity in disease characteristics and uniform mixing within the population. While admirably simple, SEIR models neglect stochasticity, demographic heterogeneity, and the structure of contact networks (20, 21). Accounting for these factors is particularly important when evaluating control strategies that can be thought of as perturbing the contact network (e.g., social distancing) or making use of it (e.g., contact tracing). In addition, pre-symptomatic and asymptomatic SARS-CoV-2 transmission are important disease characteristics that need to be incorporated into any model of the current pandemic. Finally, models based on differential equations track a deterministic average of the dynamics. For disease control, especially in smaller populations, it is important to model stochasticity to understand the distribution of potential outcomes.

In order to incorporate these important aspects of disease dynamics, we use the SEIRS+ modeling framework to implement an extended SEIR model of SARS-CoV-2 transmission in schools. In this model, a susceptible (S) member of the population becomes infected (exposed) when making a transmissive contact with an infectious individual. Newly exposed (E) individuals undergo a latent period, during which time they are not contagious as the virus is replicating but not yet shedding. Infected individuals then progress to a pre-symptomatic infectious state (I_{pre}), in which they are contagious but not yet presenting symptoms. Some infectious individuals go on to develop symptoms (I_{sym}); others remain asymptomatic while continuing to be contagious (I_{asym}). At the conclusion of the infectious period, infected individuals enter the recovered state (R) and are no longer contagious or susceptible to infection. The disease dynamics are summarized in Figure 1, described in more detail in Appendix A.1, and parameterized in Appendix A.2.1.

The SEIRS+ framework supports the implementation of extended SEIR models on stochastic dynamical networks. Individuals are represented as nodes in a contact network, allowing us to model explicitly both interaction patterns and application of interventions. In addition, parameters, interactions, and interventions can be specified on an individual-by-individual basis. This allows us to model realistic heterogeneities in disease, transmission, and behavioral parameters, which

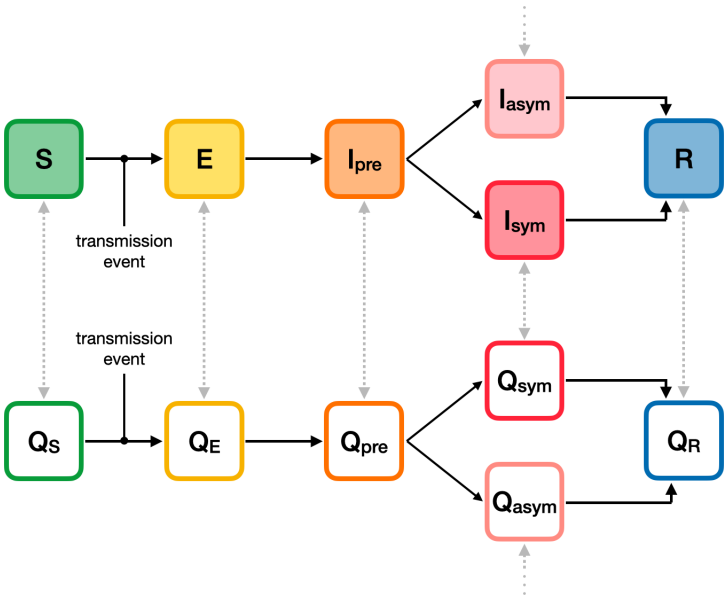

Figure 1: Compartment model. The progression of disease states in the Extended SEIR Network Model is represented by the compartments shown. Shaded compartments (top) represent susceptible (S), exposed (E), pre-symptomatic infectious (I_{pre}), symptomatic infectious (I_{sym}), asymptomatic infectious (I_{asym}), and recovered (R) members of the population. The unshaded compartments represent quarantined individuals in the respective disease states.

are particularly important when considering SARS-CoV-2 transmission dynamics in small, age-stratified school populations.

In the SEIRS+ model, the likelihood that a given susceptible individual becomes infected is proportional to the product of the prevalence of infectious individuals among their contacts, the transmissibilities of their infectious contacts, and their own susceptibility to infection (Appendix A.1.4). An individual's transmissibility (i.e., transmission rate) is equal to the expected number of cases that this individual would generate in a fully-susceptible population (i.e., the individual reproduction number) divided by the length of their infectious period. We assume an over-dispersed distribution of individual variation in transmissibility (Appendix A.2.2), which corresponds to the observation that 80% of COVID-19 transmission may be attributable to 20% of infectious individuals (22, 23). This distribution of individual transmissibility is calibrated to a nominal basic reproduction number (R_0) for the population. While the R_0 of SARS-CoV-2 varies over time and from place to place based on human behavior and social organization, many estimates land in the vicinity of 2.5-3.0 without intervention (24–28). As a baseline, we assume that schools will implement basic mitigation measures, such as mask wearing, physical distancing, and heightened hygiene, such that R_0 is reduced to 1.5 in the school population (results for other values of R_0 can be explored in the Supporting Figures). Individual susceptibility to SARS-CoV-2 infection is stratified by age, with young children less susceptible than adolescents and adults.

In standard SEIR models, individuals transition out of the exposed and infectious compartments at constant rates, and residence times in these compartments are effectively distributed according to an exponential distribution. In reality, residence times in each disease state are not exponentially distributed, and the discrepancies can be particularly important when looking at early stages of an outbreak and when considering control strategies such as proactive testing (29, 30). In the SEIRS+ framework, transmission events are stochastic rather than deterministic, and individuals can be assigned heterogeneous residence times for exposed and infectious states according to specified distributions that can take any form. Here we estimate these distributions from empirical studies (Appendix A.2.1).

Individuals may enter isolation due to symptoms or in response to a positive test result. The effect of isolating individuals is modeled by introducing compartments that represent quarantined individuals (Figure 1). An individual may be isolated in any disease state, and every disease state has a corresponding quarantine compartment. Quarantined individuals follow the same progression through the disease states, but they do not make transmissive contact with individuals outside of the home (See the Contact network structures section below and Appendix A.2.3.3). Individuals remain in quarantine for 10 days (31), at which time they transition to the non-quarantine compartment corresponding to their present disease state. Here we assume that 20% of symptomatic individuals self-isolate upon the onset of symptoms. Proactive testing and isolation are described further below.

Additional description of the Extended SEIR Network Model can be found in Appendix A.1. Extensive documentation and code for the SEIRS+ framework and the Extended SEIR Network Model can be found at https://github.com/ryansmcgee/seirsplus. Specific considerations for the primary and secondary school models are described below and detailed in Appendix A.2.

Model considerations for primary schools versus secondary schools

The dynamics of COVID-19 transmission differ substantially between primary schools and secondary schools for two principal reasons. First, children under age 10 appear to have different epidemiological characteristics of infection than do adolescents 10-19 years of age. A recent meta-analysis showed that younger children have lower susceptibility to SARS-CoV-2 infection and are about half as likely to become infected compared to adults (32). Younger children are also more likely to experience asymptomatic or mild disease than adults are (33, 34). Second, primary and secondary schools have different organizational structures. Primary schools are structured into more stable groups, with each group of students assigned to a single teacher for the entire day. By contrast, secondary school students typically move from classroom to classroom and thus encounter multiple teachers and groups of students over the course of a single day.

Primary schools appear to have a lower risk of transmission compared to secondary schools

(35–37). For example, in Israel, all schools were shut down again shortly after reopening because of a large outbreak in a secondary school. However, no cases were reported in primary schools (36). In New York, between Aug. 31 and Nov. 22, 2020, the case rate for students in primary schools was substantially lower than the case rates reported in teachers and staff and the surrounding community (7.0 vs 19.0 vs 15.0 daily cases per 100,000, respectively) (38). Meanwhile the student case rate in high schools was almost double the case rate found in primary school students (13.0 vs 7.0 daily cases per 100,000, respectively) and was similar to the case rates reported in teachers and staff and the surrounding community (16.0 vs 15.0 daily cases per 100,000, respectively) (38). Case studies of school systems in Italy and the United Kingdom found a higher proportion of case introductions resulting in school transmission and larger outbreak sizes in secondary schools compared to primary schools (37). While such reports are merely individual snapshots from a widespread and ongoing pandemic, these trends support the notion that transmission occurs less frequently in primary school students compared to those in secondary schools and the surrounding community.

To account for this, we developed two distinct models for primary and secondary schools, each with parameters chosen to reflect these critical differences (Appendix A.2). In the analysis presented here, we consider scenarios wherein primary school children are 60% as susceptible as adults, and secondary school students have the same susceptibility as adults. We also define distinct contact networks for primary and secondary schools that represent the differences in social structures between these populations, as described in the following section.

Contact network structures

In the SEIRS+ framework, infection is transmitted largely along a contact network that describes the set of close contacts for each individual in the population. Close contacts are individuals with whom one has repeated, sustained, or close-proximity interactions on a regular basis: classmates, friends, housemates, or other close relationships. In contrast, casual contacts are individuals with whom one has incidental, brief, or superficial contact on an infrequent basis and to whom one is not connected directly on the network. Disease transmission may occur either from close contacts along the network structure or from casual contacts. A network locality parameter sets the relative frequency and weight of transmission among close (local network) and casual (global) contacts in the model population (Appendix A.1.4). In both primary and secondary school settings, we assume that 80% of transmission occurs between close contacts specified by the networks. Exposure to the community is modeled by randomly introducing new cases to the school population at a rate that corresponds to the community prevalence (See the Community prevalence and case introduction rate section below).

For our primary school model, we simulate a school with 480 students, 24 teachers, and 24

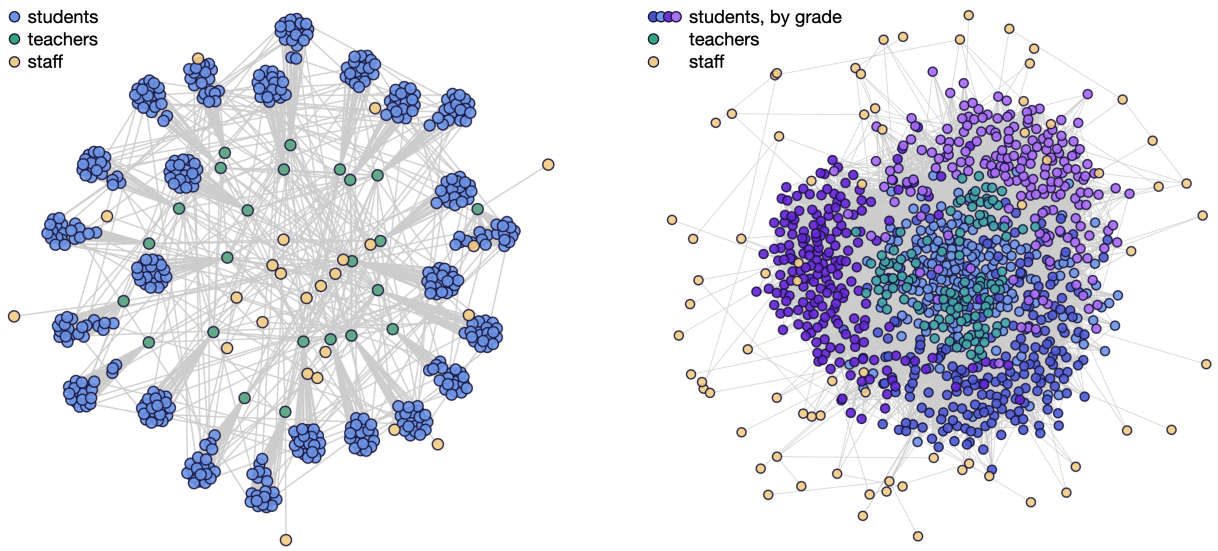

Figure 2: Network structures for primary and secondary schools. Each individual is represented by a circle, and grey lines connect close contacts. (**Left**) Primary school students (blue) are organized into classes with close contacts between all students in each classroom as well as a single teacher (green). School staff (yellow) interact with teachers and other staff. (**Right**) Secondary school students (shades of blue and purple indicating grade levels) move from classroom to classroom throughout the day and have close contact with six teachers (green) each. School staff (yellow) interact with teachers and other staff. While the secondary school network lacks the highly modular classroom structure seen in elementary schools, secondary school students are clustered into loose social groups and are more likely to interact with other students in the same grade.

additional staff. Primary school students have close contacts with their teacher, classmates, and other children in their household (e.g., siblings). For our secondary school model, we simulate a school with 800 students (200 per graduating class), 125 teachers, and 75 additional staff. Secondary school students have close contacts with six teachers, other students in their grade and social groups, and other students in their household. In addition, there is a network of close contacts among teachers and staff in both school settings. A new random network is generated for each simulation replicate. Detailed descriptions of the contact network structures and their generation can be found in the Appendix A.2.3. Example network diagrams for each school setting are shown in Figure 2.

Community prevalence and case introduction rate

The US Centers for Disease Control and Prevention (CDC) has issued guidance that emphasizes the community prevalence of cases as an important indicator for the risk of introduction and transmission of COVID-19 in schools (39). As community transmission becomes more frequent and cases become more prevalent, members of the school population are expected to become infected at a higher rate, and the risk of an outbreak increases. To account for the effect of community preva-

lence on COVID-19 dynamics in schools, we model scenarios in which new cases are introduced into the school population stochastically according to a Poisson process at rates corresponding to daily, weekly, or monthly introductions on average. When the effective community reproduction number R_{eff} is in the 1.0–2.0 range, these rates approximately correspond to the community prevalences shown in Table 1. We also consider the consequences of a single introduction so as to understand the dynamics of a single outbreak in isolation. In the single introduction scenario, all replicates start off with the case introduction occurring on the first day of the simulation.

	Corresponding Community Prevalence	
Introduction rate (Poisson λ)	Primary school (528 individuals)	Secondary school (1000 individuals)
Monthly (λ = 1/30)	0.02 - 0.04%	0.01 - 0.02%
Weekly (λ = 1/7)	0.1 - 0.2%	0.05 - 0.1%
Daily (λ = 1)	0.5 - 1%	0.25 - 0.5%

For R_{eff} in the 1.0–2.0 range.

Table 1: Introduction rates and community prevalences. Given community transmission in the range of R_{eff} = 1.0–2.0, this table relates the prevalence of disease in the community to the frequency at which new cases are introduced into a school. Details of how these ranges are estimated are provided in Appendix A.2.4.

Simulations

To account for stochastic variability in possible outcomes, we run 1,000 replicates for each parameter set. Each simulation tracks the progression of an outbreak that begins with the introduction of a single infected individual in an otherwise disease-free school population. The simulation begins on a random day of the week with the introduction of an initial case. Additional case introductions may occur randomly throughout the simulation at a Poisson rate corresponding to the level of community prevalence. School is in session 5 days a week, and it is assumed that no close contacts are made outside of the household on weekends while "global" transmission among casual contacts remains possible. The simulation proceeds for 150 days, representing a semester of schooling.

We display results from 1,000 stochastic simulations for each condition in the form of a jitter plot. To allow ready comparison across scenarios with different community prevalences, we report the percentage of individuals with cases attributable to transmissions within the school population (i.e., excluding introduced cases attributable to exogenous community exposure). These transmissions may occur either at school or among school-affiliated individuals while they are off campus, and are hereafter collectively described as "school transmission". Under each jitter distribution we display the fraction of simulation runs that result in "sizable outbreaks", with more

than 5% of the school population becoming infected in school over the course of the semester (150 days). While schools that are experiencing outbreaks are likely to stop in-person learning before very large case counts are realized, these data provide information about the probability of severe outbreak trajectories that will require such action.

Results

The effect of community prevalence

The prevalence of COVID-19 in the community is a critical driver of school transmission. Figure 3 shows the percentage of the school population infected in primary and secondary schools over the course of a semester. In these scenarios, basic distancing, hygiene, and mask wearing interventions are in place so that the basic reproduction number R_0 is 1.5, but the other interventions we consider here—testing, cohorting, classroom isolation, and vaccination—have not been deployed. Higher COVID-19 prevalence in a community increases the probability that a large number of people will be infected in primary and secondary schools alike. When community prevalence is so high as to result in new introductions on a daily basis, our simulations suggest that even aggressive interventions cannot prevent a large fraction of teachers and students from becoming infected over

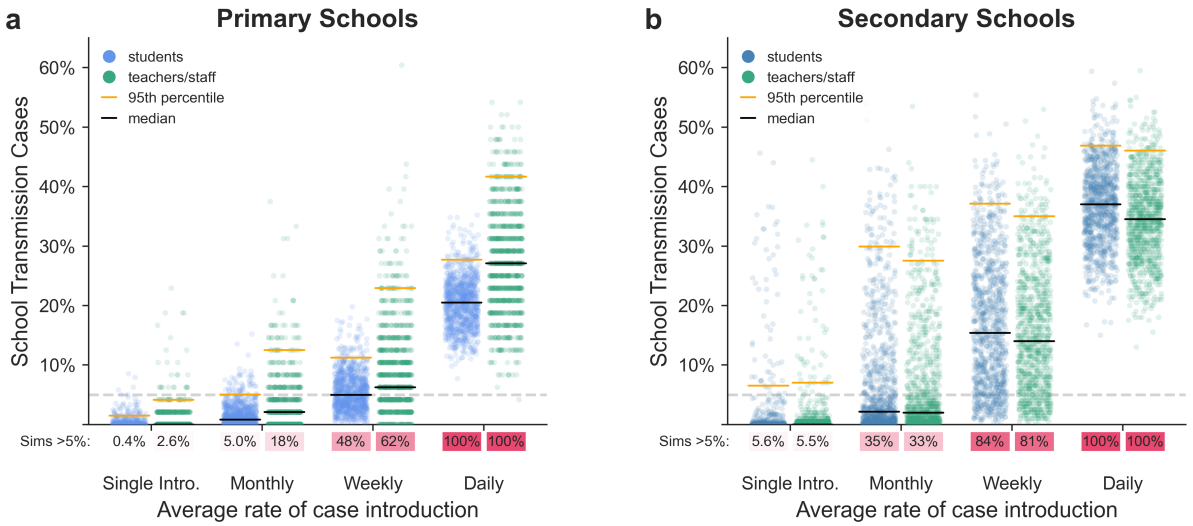

Figure 3: Effect of community prevalence. The distributions of school transmission cases as a percentage of the school population for (**a**) primary schools (size = 528 teachers, staff, and students) and (**b**) secondary schools (size = 1,000 teachers, staff, and students) under different average rates of new case introductions. In these simulations, all students are in school five days a week and there is no proactive testing. Students are indicated in blue, teachers in green. Each jitter distribution reflects the outcomes of 1,000 simulations for one specific set of conditions. Under each bar we list the percentage of simulations where more than 5% (grey dashed line) of the population are infected in school. Black and orange lines represent median and 95th percentile outcomes, respectively.

the course of a semester, in primary and secondary schools alike (Supporting Figures S1, S4, S25, S57). Of course, a full retreat to distance learning could be implemented to break chains of school-related transmission and head off the worst outcomes, at the obvious cost of interrupting or ending in-person schooling.

The probabilities of sizable outbreaks and the overall outbreak sizes are larger for secondary schools than for primary schools. This difference generally holds across the range of parameters and interventions that we explore. This is likely because secondary school students are more susceptible to the virus, and because the classroom and social structures of secondary schools result in more student-teacher contacts and more mixing among students. These results suggest that primary schools may be the most propitious for initial reopening efforts.

The effects of interventions

Proactive Testing

Proactive testing is a powerful control measure that can be used to prevent potential SARS-CoV-2 outbreaks in congregate settings such as schools (40, 41). The purpose of proactive testing is to first identify individuals who are infected but not currently showing symptoms and then isolate these individuals before they infect others. Here we consider five testing strategies, summarized in Table 2: (1) a baseline of no testing, (2) once-weekly proactive testing amongst teachers and staff only, (3) twice-weekly proactive testing amongst teachers and staff only, (4) once-weekly proactive testing cadence amongst students, teachers, and staff, and (5) twice-weekly proactive testing amongst students, teachers, and staff. We assume that 100% of teachers and staff are compliant with testing, but that 25% of students are non-compliant and thus never get tested. Test results are returned and positive individuals isolated 24 hours after being tested; previous work suggests that longer turnaround times severely curtail the value of testing (40, 42, 43). More information about how testing is implemented can be found in Appendix A.2.5.2.

Proactive Testing Cadence	Mon	Tue	Wed	Thu	Fri	Sat	Sun
No Testing							
Teachers Weekly	🟢🟡						
Teachers Semiweekly	🟢🟡			🟢🟡			
Everyone Weekly	🟢🟡🔵						
Everyone Semiweekly	🟢🟡🔵			🟢🟡🔵			

🟢 Teachers 🟡 Staff 🔵 Students

Table 2: School testing cadences. We explore the consequences of five testing cadences, from no testing to testing all members of the school community twice a week. Once-weekly testing takes place every Monday, and Semiweekly testing takes place on Mondays and Thursdays.

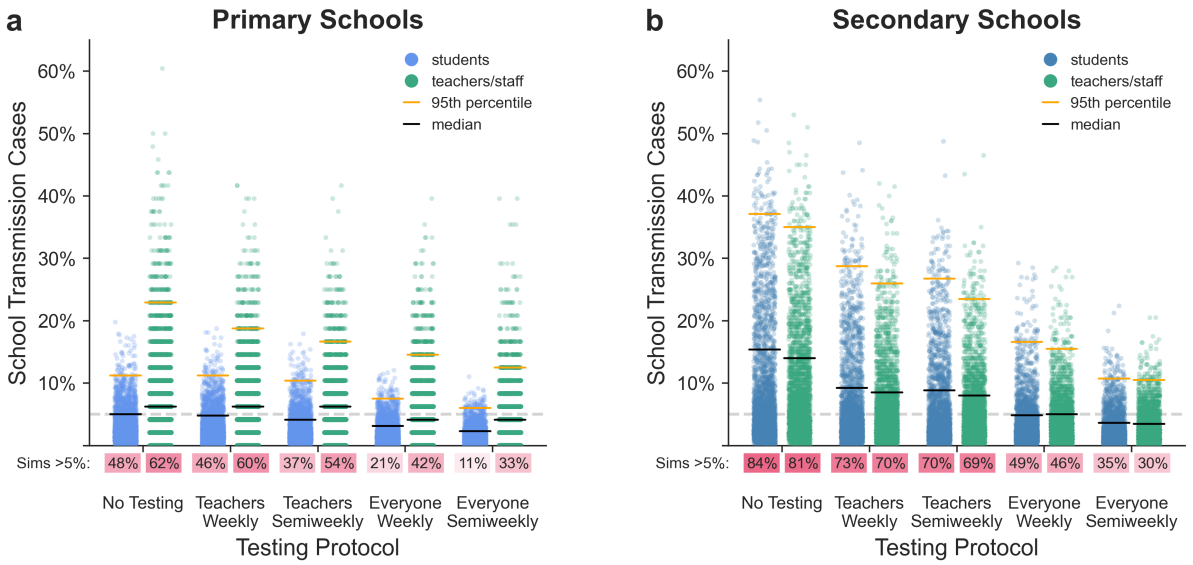

Figure 4: Proactive testing strategies. The distributions of school transmission cases as a percentage of school population for 1,000 simulations, given different proactive testing strategies in (**a**) primary schools and (**b**) secondary schools with approximately weekly new case introductions and all students on campus five days a week. Under each jitter distribution we list the percentage of simulations that result in outbreaks affecting more than 5% of the population. Black and orange lines represent median and 95th percentile outcomes respectively.

The model consistently predicts that proactive testing strategies improve outcomes. Figure 4 illustrates the effects of testing in the scenario where all students are in school five days a week and individuals (but not classrooms) are isolated upon a positive test result. More frequent testing leads to lower risk of large outbreaks in primary and secondary schools alike. Testing students and teachers once a week is substantially more effective than testing teachers twice a week — but doing so also requires four to ten times as many tests in our model, because the student populations are that much larger. Note that Figure 4 depicts the case in which introductions occur on a weekly basis. If community prevalence can be reduced to the point that introductions occur approximately monthly, sizable outbreaks become uncommon in primary schools even without testing (Supporting Figures S1, S23). In secondary schools, testing or other additional interventions remain necessary even with monthly introductions in order to keep the risk of outbreaks at low levels (Supporting Figures S4, S55).

Cohorting

Cohorting, wherein students are divided into two or more groups for in-person learning, is a common strategy for mitigating outbreak in school settings (44–46). Alternating or staggered scheduling can be used in conjunction with cohorting to further reduce risk. Using these strategies, only one cohort of students from each class is on campus at any given time, and teachers work with

each cohort in succession. In our model, we represent cohorting by shifting the contact networks according to which students are on campus (Appendix A.2.3.5). While off campus, students are disconnected from the school network but maintain household connections and global transmission (the latter representing out-of-school interactions among the student body). Teachers, on the other hand, remain on campus across all cohorts. Example network structures for student cohorting are shown in Figure 5.

Figure 6 illustrates how cohorting interacts with testing, for three common cohorting strategies: (1) all students belong to a single cohort that is on campus full time (five days a week), (2) students are divided into two cohorts, A and B, which are on campus on alternating days, and (3) students are divided into two cohorts which are on campus on alternating weeks (Appendix A.2.5.3).

We find that relative to no cohorting, alternating day and alternating week strategies can improve outcomes substantially. Cohorting with alternating weeks outperforms cohorting with alternating days, particularly in primary schools.

In primary schools, cohorting alone dramatically reduces the risk of outbreak amongst students. For the parameters illustrated in Figure 6 and in the absence of testing, the probability of an outbreak infecting more than 5% of the students plummets from nearly fifty percent with no

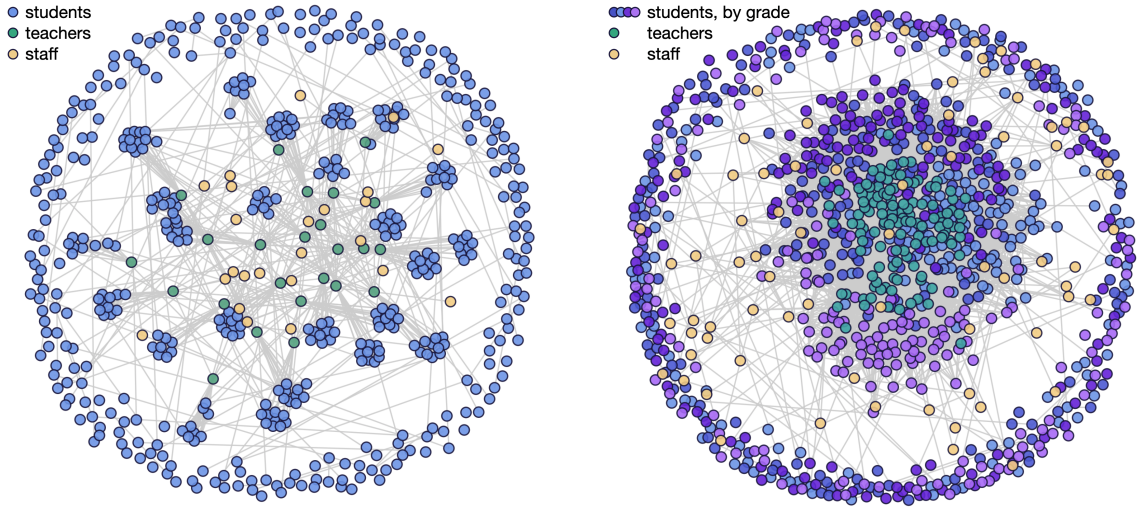

Figure 5: Network structures for student cohorting. Modified network structures used to simulate student cohorting are shown when the A cohorts are at school and the B cohorts are at home. In the primary school network (left), students in the A cohort are arranged into small classes represented by the tight clusters in the interior. Students in the B cohort are not in school and appear around the periphery of the network diagram. In the secondary school network (right), students in the A cohort are attending classes and appear in the interior, and students in the B cohort are at home and ring the periphery. Students are indicated in blues and purples and colored by grade in the secondary school network, while teachers are depicted in green and staff in yellow. Students in the B cohort have connections with housemates (visible as edges between nodes on the periphery) and can be involved in global transmission events, but not not make close contact with the rest of the school population while offsite.

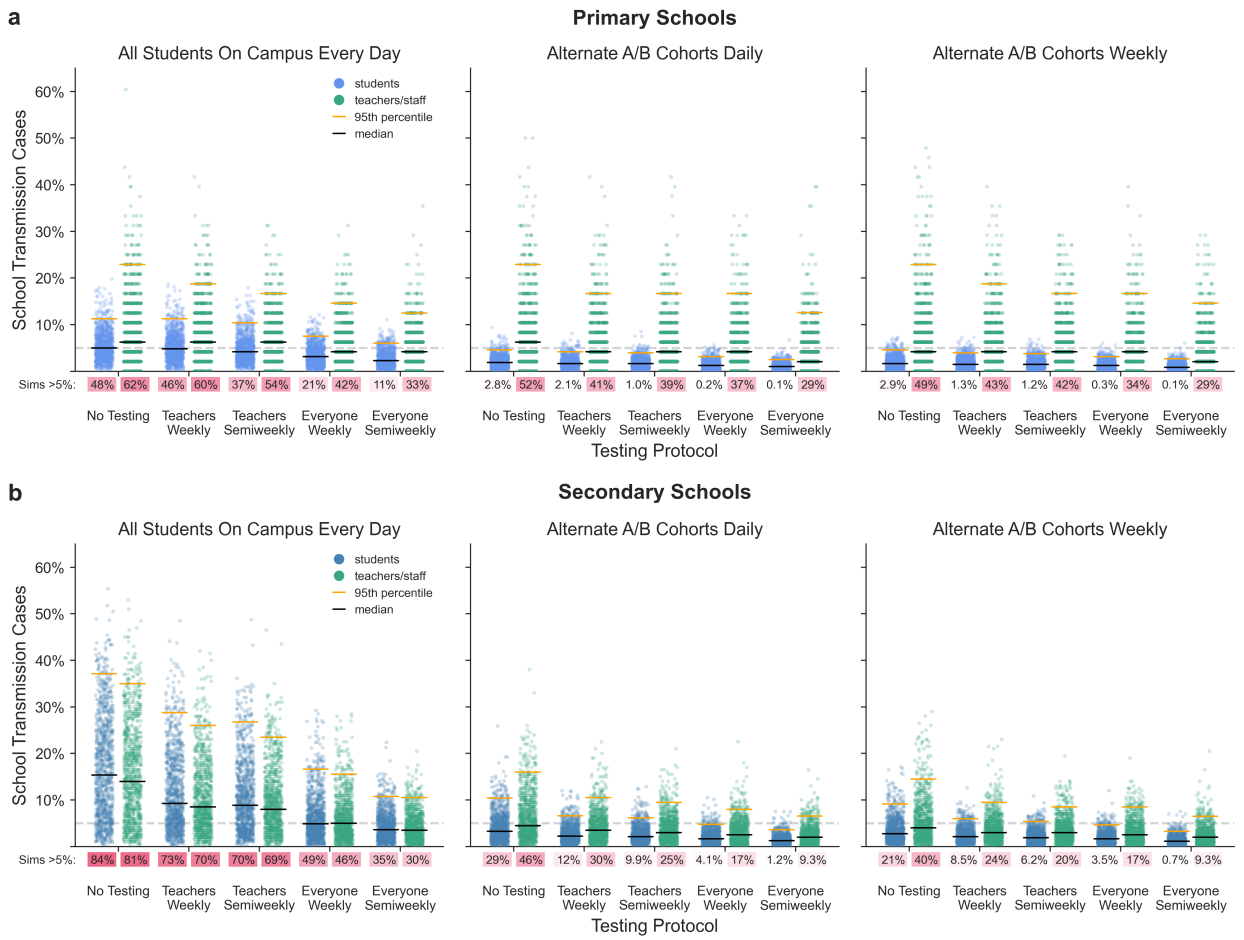

Figure 6: School Cohorting and Testing Strategies. We consider three different cohorting strategies: all students onsite all school days; two cohorts, alternating days; two cohorts, alternating weeks. Here we illustrate the distributions of school transmission cases as a percentage of the school population for 1,000 simulations of each cohorting strategy in (**a**) primary schools and (**b**) secondary schools. New cases are introduced on an approximately weekly basis. Under each jitter distribution we list the percentage of simulations that result in outbreaks affecting more than 5% of the population. Black and orange lines represent median and 95th percentile outcomes respectively.

cohorting to around three percent with weekly cohorting. Cohorting has a much smaller effect on primary school teachers and staff. Even with weekly cohorting, the risk of infecting more than 5% of the teachers and staff hovers at nearly fifty percent in the absence of testing. In the secondary schools, cohorting is helpful but is insufficient on its own to keep the likelihood of an outbreak low amongst students or amongst teachers and staff.

In practice, schools can deploy a combination of testing and cohorting. Figure 7 illustrates the interactions among these interventions in a primary school environment. Each cell in the grid is colored to indicate effect size, quantified as the log ratio of mean cases under the column treatment compared to the row treatment. Blue shades indicate that the column treatment is more effective

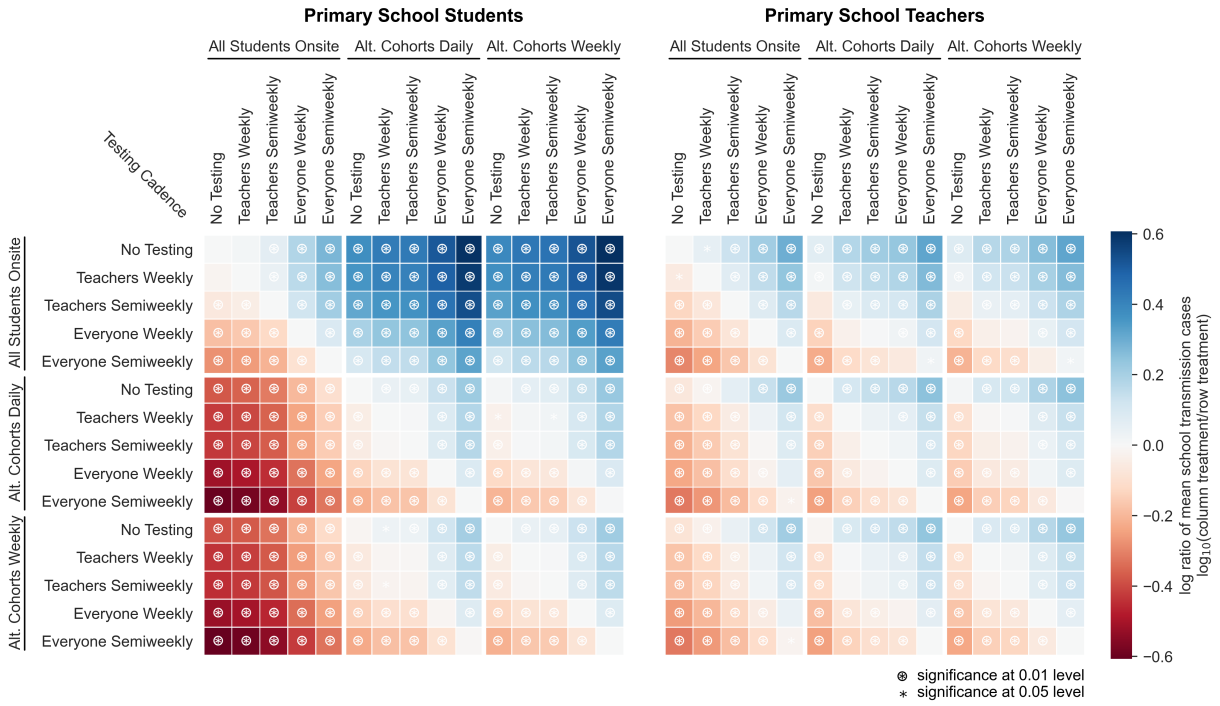

Figure 7: Relative effects of testing and cohorting in a primary school setting. A heatmap of pairwise comparisons of testing and cohorting interventions illustrates the effects of various interventions on mean outbreak sizes. Introductions occur weekly on average, and when a case is detected by testing, only the positive individual is isolated. Each cell is colored according to the log ratio of mean outbreak sizes for the two interventions, which represents the effect of the column intervention relative to the row intervention (i.e., a blue cell indicates that the column intervention achieves a lower mean outbreak size than the row intervention). Symbols in cells denote statistically significant differences in outbreak size distributions according to the Mann-Whitney U test at the 0.01 (⊛) and 0.05 (∗) levels.

than the row treatment; red shades indicate the reverse. Symbols overlaid on each square indicate the significance of these differences according to a Mann-Whitney U test. The grid at left shows the relative effects of interventions on cases among students; the grid at right shows the effects on cases among teachers.

The left-hand panel in Figure 7 reveals that more aggressive testing helps reduce the size of outbreaks, as does more aggressive cohorting. Cohorting on alternating weeks outperforms cohorting on alternating days, which in turn outperforms no cohorting. In addition to showing the general benefits of each intervention on its own, the diagram illustrates that testing and cohorting together outperform either measure alone.

Individual interventions that help students also help teachers, and vice versa. Holding cohorting constant, any change in testing with a statistically significant effect has the same direction of effect on students as on teachers. Likewise, and holding testing constant, any change in cohorting with a statistically significant effect has the same direction of effect on both groups. However, specific interventions may help one group more than another. Unsurprisingly, increasing testing teachers

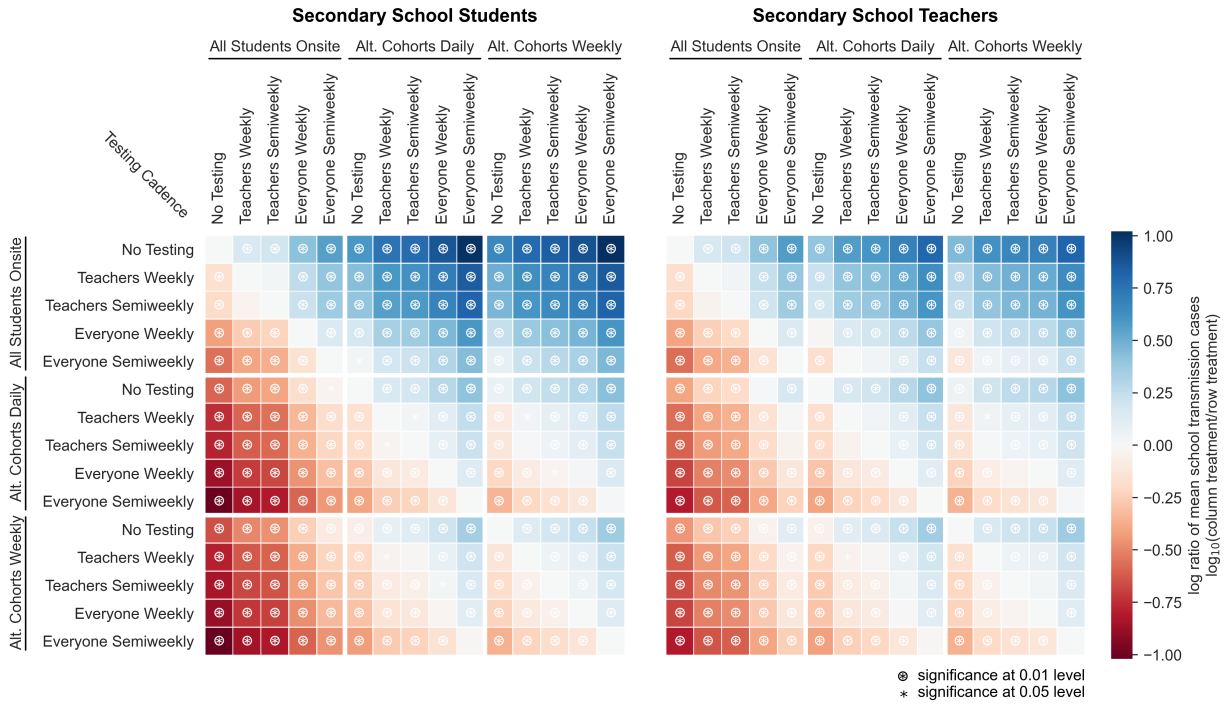

Figure 8: Relative effects of testing and cohorting in a secondary school setting. A heatmap of pairwise comparisons of testing and cohorting interventions illustrates the effects of various combinations on mean outbreak sizes. Introductions are weekly on average, and when cases are detected only the positive individual is isolated. Each cell is colored according to the log-ratio of mean outbreak sizes for the two interventions, which represents the effect of the column intervention relative to the row intervention (i.e., a blue cell indicates that the column intervention achieves a lower mean outbreak size than the row intervention). Symbols in cells denote statistically significant differences in outbreak size distributions according to the Mann-Whitney U test at the 0.01 (⊛) and 0.05 (∗) levels.

confers greater marginal benefits on teachers than it does on students. This is likely because the teacher population is enriched for cases relative due to the higher susceptibility and higher connectivity of teachers relative to students in primary schools. Cohorting, by contrast, helps students more than teachers. Teachers remain on campus five days a week whether cohorting is practiced or not, whereas students spend half of their time at home with minimal exposure under a cohorting plan.

Because of these differences in relative effect, a few pairs of changes have opposite consequences for the two groups. Suppose a school is cohorting on a daily basis but is not testing. If the school switches to having students on-site five days a week and tries to compensate by testing students and teachers twice weekly, students will end up worse off, but the teachers will be better off. This is because students benefit a lot from cohorting, but teachers do not—so the cost to the former of switching to a full-time schedule is higher.

Figure 8 illustrates the interaction among interventions in a secondary school environment. The patterns are generally similar to those in a primary school setting, but the effect sizes in secondary

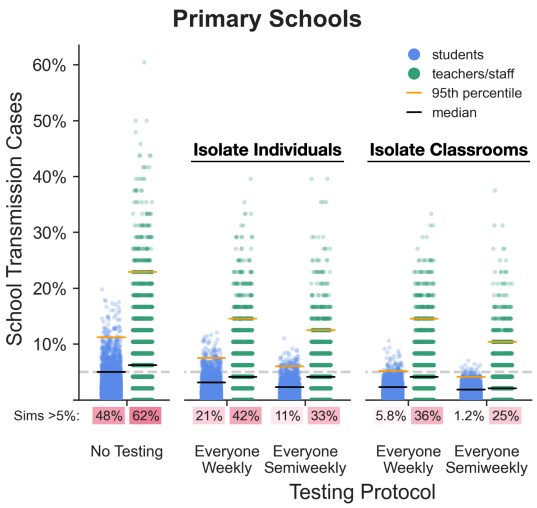

Figure 9: Effect of isolating classrooms. We consider two quarantine strategies for primary schools: (1) isolate single individuals who receive a positive test result, and (2) isolate the entire classroom (students and teacher) associated with an individual who receives a positive test. The distributions of school transmission cases as a percentage of the school population are shown for 1,000 simulations of each testing and isolation strategy. New cases are introduced on an approximately weekly basis. Under each jitter distribution we list the percentage of simulations that result in outbreaks affecting more than 5% of the population. Black and orange lines represent median and 95th percentile outcomes respectively.

schools are substantially larger than those in primary schools—note the different color scales of the heatmaps— presumably because higher case counts in secondary school settings offer more room for improvement. In addition, the magnitude of the benefit that teachers get from more aggressive interventions is larger in secondary schools relative to primary schools, because secondary school teachers are more highly connected to a population that is itself more mixed and more susceptible to transmission.

Isolation protocols

When an infected individual is identified by proactive testing, that person should be immediately isolated to prevent further transmission. In primary schools where classroom organization is stable, school administrators may additionally consider quarantining the entire classroom—students and teacher—with which an infected individual was associated.

Our model indicates that classroom-level quarantine is more effective than individual quarantine (Figure 9). For students and for teachers, under both weekly and semiweekly testing, the distribution of outcomes from isolating classrooms is significantly better than that from isolating individuals when new cases enter the school approximately weekly (Mann-Whitney U test, $p \ll 0.01$). However, there is not always a statistically significant benefit from isolating classrooms when cases enter the school more infrequently. One important consideration for quarantin-

ing at the classroom-level is the total number of quarantine days that will be experienced across the cohort. Obviously, when you quarantine an entire classroom in response to a positive case, you impose a much larger number of quarantine days. When choosing between an individual-based or classroom-based quarantine strategy, the cost benefit of in-person learning days lost, both by students and by teachers, should be taken into account.

Vaccination

Pfizer-BioNTech and Moderna have reported extremely encouraging results from their phase III COVID-19 vaccine trials, with 90% or greater efficacy at blocking symptomatic disease (47, 48). Distribution of both vaccines are underway in the US. Other vaccines may also be close behind in the pipeline. Guidance from the US Advisory Committee on Immunization Practices has recommended that first available doses of the vaccine be distributed to healthcare personnel and residents in long-term care facilities (49). As more vaccine doses become available, it is likely that vaccination programs will be expanded to essential workers, including school teachers and staff. A recent UNICEF statement urged that teachers be prioritized for vaccination (after frontline workers) to help protect them from infection and to allow schools to reopen for in-person learning (50).

Some vaccines, such as those for measles, block infection, disease, and transmission. Others, such as the pneumococcal (bacterial pneumonia) conjugate vaccine and the acellular pertussis (whooping cough) vaccine, block disease but may have a limited effect on transmission. Because all COVID-19 vaccine trial data to date have focused only on diagnosis of symptomatic disease as a primary endpoint, we do not know the degree to which COVID-19 vaccines block transmission. As such, we consider multiple scenarios for post-vaccination transmissibility in the model (Figure 10).

As expected, our model predicts that when teachers and staff are vaccinated against COVID-19 with a 90% effective vaccine, this group is well-protected against infection (see Appendix A.2.5.5 for more information about vaccination in the model). (Even with vaccination we do see some cases among teachers and staff, simply because we are assuming only 90% effectiveness). A more surprising result is the degree to which vaccinating teachers with a transmission-blocking vaccine can reduce the risk of outbreaks among secondary school students, particularly when paired with cohorting. In primary schools where students have fewer teacher contacts, such effects are more modest. In primary and secondary schools alike, students receive some benefit from vaccinating teachers even if the vaccine only partially reduces transmissibility, but vaccinating teachers alone is not enough to eliminate risk in the student population without additional intervention. While vaccination benefits those who have been vaccinated and facilitates reopening overall, maintaining additional interventions will be particularly important if vaccines turn out to be only partially effective at blocking transmission.

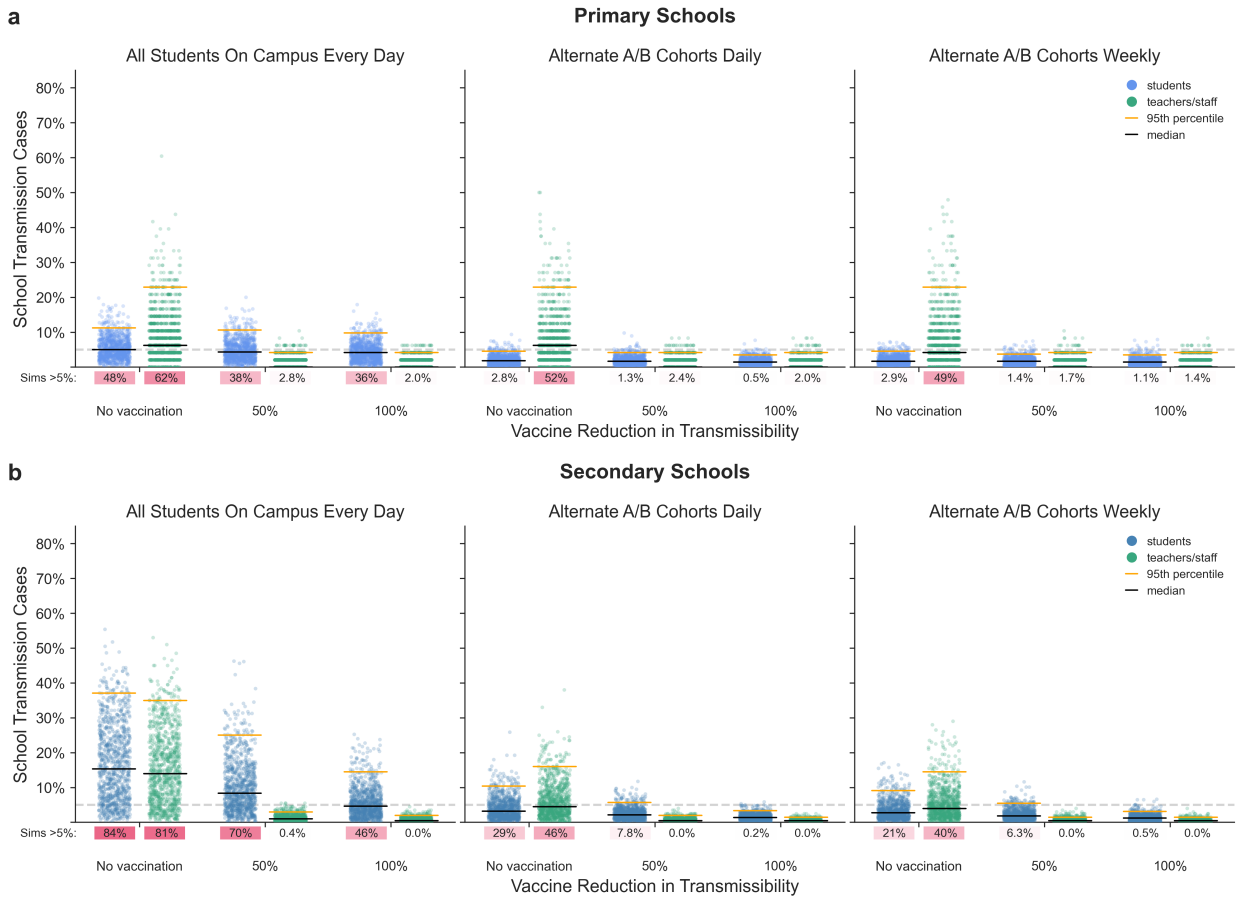

Figure 10: Effects of vaccinating teachers. The distribution of model outcomes when all teachers and staff are vaccinated is compared to the distribution of outcomes when no one is vaccinated. We consider vaccines that block transmission fully (100% reduction in individual transmissibility) or only partially (50% reduction in individual transmissibility). We show results for vaccination in the setting of three cohorting strategies but in the absence of testing. Results are shown for (a) primary schools and (b) secondary schools with new cases introduced approximately weekly. We illustrate the distributions of school transmission cases from 1,000 simulations as a percentage of the school population. Because vaccination is only 90% effective, some teachers and staff become infected even when all are vaccinated. Under each jitter distribution we list the percentage of simulations that result in outbreaks affecting more than 5% of the population.

Novel high-transmissibility strains

As of January 2021, several SARS-CoV-2 variants appear to have evolved higher transmissibility relative to their ancestors (7). For example, the B.1.1.7 lineage that has spread throughout the UK appears to be 30%-70% more transmissible than previous SARS-CoV-2 variants (7, 51, 52). Should the B.1.1.7 variant or other more transmissible strains become predominant in a locale, this could be a serious setback for school reopening plans. To understand how highly transmissible variants might impact transmission dynamics in schools we look at the consequences of a 50%

increase in transmissibility, which increases the assumed baseline R_0 for the school environment from R_0=1.5 to R_0=2.25. These results reflect environments where highly transmissible strains have become predominant. Results for more incremental increases in mean transmission rates that approximate intermediate penetrance of such strains can be found in the Supporting Figures.

Figure 11 illustrates how community prevalence, as modeled by introduction rate, influences school transmissions when schools are confronted by this more transmissible strain. Even under a monthly rate of new case introductions, schools face the risk of a major outbreak. With more frequent introductions, substantive outbreaks become the most likely outcome. Figure 12 shows the impact of control measures on a more transmissible strain with approximately weekly new case introductions. Aggressive controls mitigate the risk somewhat, but are considerably less effective for a strain with R_0=2.25 than for a strain with R_0=1.5.

Because highly transmissible variants such as B.1.1.7 pose increased risks for outbreaks, schools need to be vigilant on multiple fronts. First, where genomic surveillance is available, school districts and counties need to monitor the introduction and spread of these variants. Second, irrespective of the variants involved, it will be important to monitor epidemic dynamics within any given school and to respond quickly should uncontrolled spread take place. An additional virtue of testing is that it facilitates early detection of such events. Our model suggests that under certain parameters, a full retreat to distance learning may be necessary to avoid a substantial percentage of both students and teachers becoming infected.

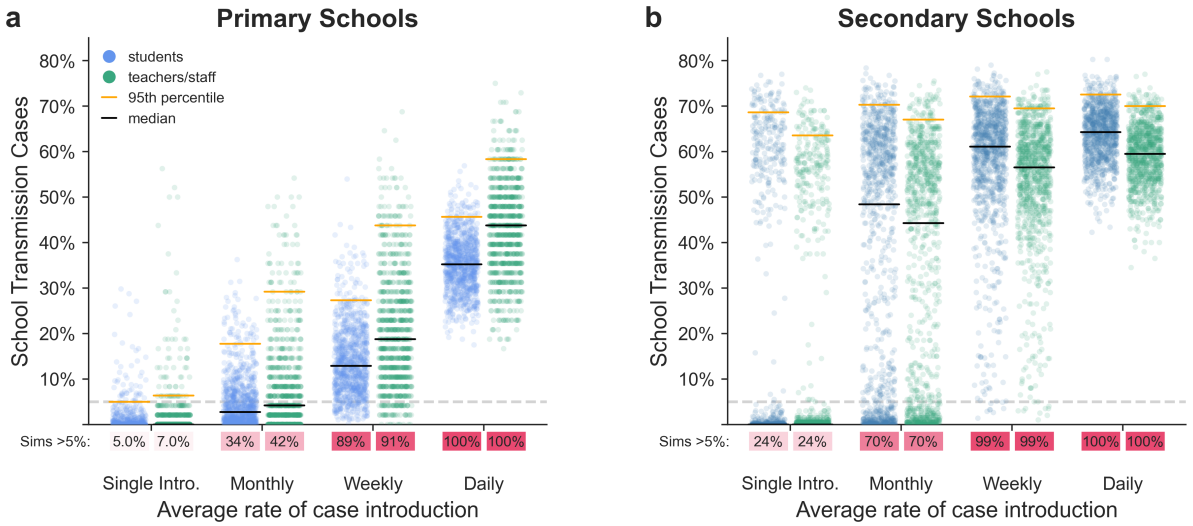

Figure 11: Effect of community prevalence rate for a highly-transmissible variant. When R_0 is increased from 1.5 to 2.25 to reflect the presence of a more transmissible variant such as B.1.1.7, large outbreaks become common at lower introduction rates. Here we show the fraction infected over a semester with everyone in school 5 days a week and no testing.

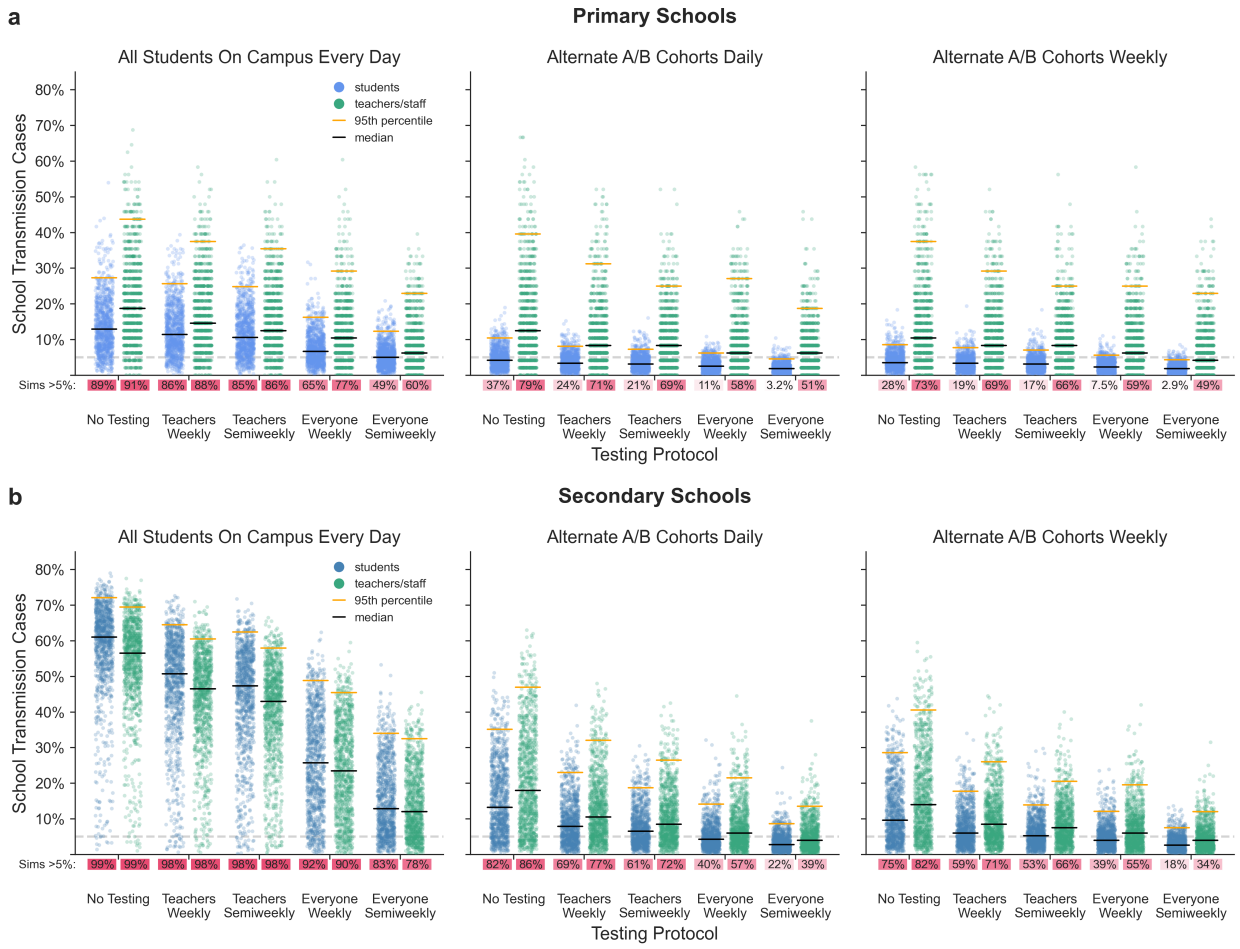

Figure 12: Effects of control measures on a highly-transmissible variant. New case introductions occur on an approximately weekly basis. When R_0 is increased from 1.5 to 2.25, more aggressive control measures are necessary to mitigate risk.

Limitations

Like all epidemiological models, ours is a simplification of a complex, highly variable world. Our model is built on a series of assumptions and parameters based on the available evidence at the time of publication. To the degree that those assumptions do not accurately reflect the epidemiological dynamics or social structure in the real world, the model will be ineffective at predicting even the range of possible outcomes. We have attempted to account for uncertainty by embracing realistic heterogeneity and stochasticity in our model and by evaluating the sensitivity of outcomes across plausible ranges of values for critical parameters (see the Supporting Figures). Still, in a novel pandemic where many epidemiological parameters remain uncertain, and social and behavioral factors are fluid, some mismatch is inevitable.

The basic reproduction number (R_0)—the average number of new cases generated by an infec-

tious individual in a fully susceptible population—is a critical parameter with strong effects on the dynamics and outcomes observed in all epidemiological models. At the time of writing, the effective reproduction number is in the range 1.0-1.2 for many communities in the United States (53). This reflects an average rate of transmission integrated over many contexts and behaviors, including widespread efforts to curtail transmission, such as social distancing, restricting large groups, and closing many schools, businesses, and other gathering places. Reopening schools would reintroduce settings where large numbers of individuals interact, and it is reasonable to imagine that average rates of transmission could be higher in schools than in the overall community in the absence of further mitigation efforts. Still, basic in-school interventions such as mask wearing, physical distancing, and behavioral changes are expected to significantly reduce R_0.

In our model, we assume that these basic measures can reduce R_0 to 1.5, roughly half of what it would be in the absence of intervention. Previous studies suggest that transmission is relatively limited in schools (34, 45, 46, 54–56). Many of the schools described in these studies were already implementing one or more interventions along the lines of the ones we analyze here: cohorting, isolating groups, testing, contact tracing, reducing the number of people on campus, and so forth (37, 45, 56, 57). These studies largely corroborate our findings that school transmission is often kept in check when such mitigation strategies are used. Fewer studies have considered schools that are only using masks and other basic measures, but there is evidence that sizable school outbreaks can occur in these contexts (36). Our choice of a baseline R_0=1.5 reflects our assumption that transmission is reduced but non-negligible in school settings where coordinated mitigation strategies such as testing and cohorting have not been deployed. We find that the probability and size of outbreaks are influenced by the underlying R_0, but the relative effects of mitigations are robust across a range of R_0 values (Supporting Figures).

Here we have simulated a subset of the currently recommended strategies for returning to in-person learning (58). We assume that students, teachers and school staff adhere to testing cadences, cohorting schedules, and isolation policies in addition to basic interventions such as physical distancing, mask wearing, and good hygiene. We did not investigate how variations in compliance with these strategies or how the use of other mitigation strategies not discussed here could impact transmission. In the absence of evidence to the contrary, we assume that—holding transmissibility and susceptibility constant—all forms of close contact are equally likely to result in transmission. In practice, the nature of interpersonal relations may make transmission from student to student or from teacher to teacher more likely than transmission between these groups, and could explain why some contact-tracing studies have reported disproportionately low student-to-teacher transmission (45, 59).

In our analysis, we model primary school children (age 10 and below) as being less susceptible to SARS-CoV-2 infection than are teachers and staff. Recent evidence from seroprevalence

and contact-tracing studies support this assumption (32, 35, 60–62). However, because a high percentage of children develop asymptomatic disease, COVID-19 cases among children may be more likely to go undetected. Therefore, it is possible that the apparent decreased susceptibility to SARS-CoV-2 infection among primary school aged children is an artifact of asymptomatic cases in children going undetected and underreported. If young children are similarly susceptible to adults, the risk of transmission in primary schools will be higher.

We assume a constant hazard of community introductions throughout the duration of the simulation. In practice, community prevalences nearly everywhere have fluctuated substantially over a timescale of a few months. Because these fluctuations are due to changing individual behaviors and societal interventions in ways that have been largely unpredictable, we do not have a ready avenue to incorporate these fluctuations into our model and have elected to use a constant introduction rate.

In assuming a constant hazard of introduction, we are effectively decoupling infection dynamics within the school from epidemic dynamics in the community. In our model, intervention choices that lead to a large number of transmissions in some or all of the schools within a community do not feed back on the community prevalence to influence the downstream hazard of community introduction back into the school. Similarly, in our model, mitigation choices that block school transmission do not reduce the community introduction rate. This seems reasonable when schools are not important drivers of the community prevalence of SARS-CoV-2 infection, as appears to be the case especially for K-5 schools (37, 45, 63). Where schools are important drivers of community dynamics, however, our model risks underestimating the consequences of effective or ineffective mitigation in the schools. When schools drive community prevalence, planners must also consider the cost of the additional community infections that result from reopening schools—which we have not done here.

Discussion

We have presented results from a simulation model of reopening schools during the COVID-19 pandemic. The purpose of this model is to provide a scenario-simulating tool that, when used in concert along with other credible sources of information and data, can aid policymakers and administrators in their decisions around school reopening policies.

Because chance plays a large role in outbreaks, two schools with very similar characteristics and mitigation plans may experience substantially different outcomes. We attempt to capture this with the stochastic nature of our model. For each scenario we illustrate the range of likely outcomes, rather than predicting a specific result. Additional uncertainty arises in the form of epidemiological parameters that remain unknown, and through unpredictable and dynamically changing

aspects of human behavior. We attempt to make the most reasonable assumptions about both of these domains. To the degree that our assumptions are off, the model's predictions will be inexact. Even where this happens, the qualitative predictions of a well-structured model are often robust to misestimation of parameters, and the general trends that we observe here — advantages to cohorting, testing, and vaccination — are likely to hold up more broadly (Supporting Figures).

The success of reopening efforts will hinge on the amount of transmission that occurs in schools. The higher the transmissibility, parameterized here as R_0, the greater the chance of substantial outbreaks in a school setting. Social distancing, diligent use of masks, and other environmental controls offer a first-line approach to reducing transmission and will be an important component of reopening plans.

Our model suggests that dividing students into two stable cohorts that attend school in-person on alternating schedules can be a powerful strategy for mitigating risk. Student cohorting is a more effective strategy in primary schools compared to secondary schools, due to the more stable classroom organization. Secondary schools could consider restructuring classroom organization to reduce the mixing of students between classrooms, and thereby mimic the stable cohorts of primary schools to increase the effectiveness of cohorting. Note that cohorting is effective in our model because students largely restrict in-person interactions to other individuals within their own groups, and this takes place only while at school. When students socialize across cohort boundaries outside of school—as secondary students are wont to do—the protective effect of cohorting is reduced.

Compared to students, teachers and staff are at higher risk for more severe disease and, in primary schools, pose a higher risk of spreading the virus. Moreover, teachers serve as conduits for outbreaks to move among classrooms within the school network. Frequent, proactive testing of teachers and staff can interrupt such transmission chains and further protect them from infection.

Vaccinating teachers and staff is a powerful tool for protecting this critical workforce. If vaccines effectively block SARS-CoV-2 transmission in addition to COVID-19 symptoms, vaccinating teachers and staff can significantly dampen outbreak dynamics in both primary and secondary schools. The result would be fewer cases among adults and students alike. These factors merit consideration when determining vaccination priority for teachers and school staff.

For both primary and secondary schools, the risk of an outbreak increases as cases in the surrounding community rise. One of the most effective ways to safely reopen schools is by controlling COVID-19 in the community. Because schools will need to respond flexibly to the prevalence of disease in the surrounding community, surveillance should be in place to continuously monitor levels of community transmission and facilitate timely interventions. For example, schools could plan to increase the intensity of mitigation effectors in response to increasing community prevalence or transmission rates.

The emergence and spread of new highly transmissible SARS-CoV-2 strains, such as the B.1.1.7 lineage, will result in higher burden of cases within the community, as well as higher chances of outbreaks within schools. Where such strains become predominant, we expect both the risk and sizes of school outbreaks to increase.

Under some circumstances it may become difficult or impossible to keep the probability of outbreaks low across the schools of an entire district. Trip-wire strategies may be necessary, whereby school districts return to distance learning in response to worsening conditions.

In the Supporting Figures, we provide results from our model for a range of parameter combinations, including transmissibility (R_0), case introduction rates, student susceptibilities, and intervention strategies, which can be used to assist in dynamic decision-making in response to uncertain and changing local circumstances. Our online webapp (https://www.color.com/impact-of-primary-school-covid-19-testing) provides a way to explore the range of parameters in an interactive fashion.

While gaps remain in our understanding of transmission in school settings, both real-world experience and models — including the one presented here — suggest a path forward for schools to reopen, particularly when community transmission is low and when it is possible to deploy and consistently implement the mitigation measures we have modeled here.

Acknowledgements The authors thank Martin Rosvall for help in developing the contact network structures used in the SEIRS+ model. Ted Bergstrom, Natalie Dean, Bill Hanage, Michael Lachmann, and Marc Lipsitch provided valuable feedback in developing the model and adapting it to the school scenarios considered here.

Author contributions Conceived of the model: RSM, CTB. Reviewed the literature: RSM, HEW. Parameterized the model: RSM, JRH, HEW. Implemented the model and ran the simulations: RSM, JRH. Produced the data visualizations: RSM, JRH. Analyzed the results: RSM, CTB, JRH, HEW, AYZ. Developed the interactive web app: JRH. Drafted the manuscript: CTB, RSM, HEW, JRH, AYZ.

Disclosures CTB and RSM consult for Color Health. CTB has received honoraria from Novartis. JRH, HEW and AYZ are currently employed by and have equity interest in Color Health.

References

[1] (2020) 1.3 billion learners are still affected by school or university closures, as educational institutions start reopening around the world, says UNESCO (https://en.unesco.org/news/13-billion-learners-are-still-affected-school-university-closures-educational-institutions). Accessed: 2020-11-9.

[2] Hanushek EA, Woessmann L (2020) The economic impacts of learning losses.

[3] (2020) Averting a lost COVID generation (https://www.unicef.org/reports/averting-lost-generation-covid19-world-childrens-day-2020-brief). Accessed: 2020-12-10.

[4] (2020) Taking back control: A resetting of america's response to covid-19 - the rockefeller foundation (https://www.rockefellerfoundation.org/report/a-resetting-of-americas-response-to-covid-19/). Accessed: 2021-1-5.

[5] of Pediatrics AA (2020) Covid-19 planning considerations: guidance for school re-entry. *Critical Updates on COVID-19-Clinical Guidance* 2019:1–11.

[6] National Academies of Sciences, Engineering, and Medicine; Division of Behavioral and Social Sciences and Education; Board on Children, Youth, and Families; Board on Science Education; Standing Committee on Emerging Infectious Diseases and 21st Century Health Threats; Committee on Guidance for K-12 Education on Responding to COVID-19 (2020) *Reopening K-12 Schools During the COVID-19 Pandemic: Prioritizing Health, Equity, and Communities* eds. Schweingruber H, Dibner K, Bond EC. (National Academies Press (US), Washington (DC)).

[7] Galloway SE (2021) Emergence of SARS-CoV-2 b.1.1.7 lineage — united states, december 29, 2020–january 12, 2021. *MMWR Morb. Mortal. Wkly. Rep.* 70.

[8] Nierenberg A, Pasick A (2020) Will any more schools reopen in 2020? *The New York Times*.

[9] Leidman E (2021) COVID-19 trends among persons aged 0–24 years — united states, march 1–december 12, 2020. *MMWR Morb. Mortal. Wkly. Rep.* 70.

[10] Giordano G, et al. (2020) Modelling the COVID-19 epidemic and implementation of population-wide interventions in italy. *Nat. Med.* 26(6):855–860.

[11] CDC (2021) COVID-19 forecasts: Deaths (https://www.cdc.gov/coronavirus/2019-ncov/covid-data/forecasting-us.html). Accessed: 2021-1-7.

[12] Ferguson NM (2020) *Report 9: Impact of Non-pharmaceutical Interventions (NPIs) to Reduce COVID19 Mortality and Healthcare Demand.* (Imperial College London).

[13] Kucharski AJ, et al. (2020) Early dynamics of transmission and control of COVID-19: a mathematical modelling study. *Lancet Infect. Dis.* 20(5):553–558.

[14] Peak CM, et al. (2020) Individual quarantine versus active monitoring of contacts for the mitigation of COVID-19: a modelling study. *Lancet Infect. Dis.* 20(9):1025–1033.

[15] Aleta A, et al. (2020) Modelling the impact of testing, contact tracing and household quarantine on second waves of COVID-19. *Nat Hum Behav* 4(9):964–971.

[16] Wang X, et al. (2020) Effects of cocooning on coronavirus disease rates after relaxing social distancing. *Emerg. Infect. Dis.* 26(12):3066–3068.

[17] Bershteyn A, Kim HY, McGillen JB, Braithwaite RS (2020) Which policies most effectively reduce SARS-CoV-2 transmission in schools? *medRxiv*.

[18] Bracis C, et al. (2021) Widespread testing, case isolation and contact tracing may allow safe school reopening with continued moderate physical distancing: A modeling analysis of king county, WA data. *Infect Dis Model* 6:24–35.

[19] Keeling MJ, Rohani P (2011) *Modeling Infectious Diseases in Humans and Animals*. (Princeton University Press).

[20] Danon L, House TA, Read JM, Keeling MJ (2012) Social encounter networks: collective properties and disease transmission. *Journal of The Royal Society Interface* 9(76):2826–2833. Publisher: Royal Society.

[21] Badham J, Stocker R (2010) The impact of network clustering and assortativity on epidemic behaviour. *Theoretical Population Biology* 77(1):71–75.

[22] Endo A, Abbott S, Kucharski A, Funk S (2020) Estimating the overdispersion in COVID-19 transmission using outbreak sizes outside china. wellcome open research, 5 (67).

[23] Adam D, et al. (2020) Clustering and superspreading potential of severe acute respiratory syndrome coronavirus 2 (SARS-CoV-2) infections in hong kong.

[24] Li Q, et al. (2020) Early transmission dynamics in wuhan, china, of novel Coronavirus-Infected pneumonia. *N. Engl. J. Med.* 382(13):1199–1207.

[25] (2020) Royal society publishes rapid review of the science of the reproduction number and growth rate of COVID-19 (https://royalsociety.org/news/2020/09/set-c-covid-r-rate/). Accessed: 2021-1-17.

[26] Read JM, Bridgen JRE, Cummings DAT, Ho A, Jewell CP (2020) Novel coronavirus 2019-nCoV: early estimation of epidemiological parameters and epidemic predictions.

[27] CDC (2020) Healthcare workers (https://www.cdc.gov/coronavirus/2019-ncov/hcp/planning-scenarios.html). Accessed: 2021-1-17.

[28] Liu Y, Gayle AA, Wilder-Smith A, Rocklöv J (2020) The reproductive number of COVID-19 is higher compared to SARS coronavirus. *J. Travel Med.* 27(2).

[29] Krylova O, Earn DJD (2013) Effects of the infectious period distribution on predicted transitions in childhood disease dynamics.

[30] Feng Z, Xu D, Zhao H (2007) Epidemiological models with non-exponentially distributed disease stages and applications to disease control. *Bull. Math. Biol.* 69(5):1511–1536.

[31] CDC (2020) Options to reduce quarantine for contacts of persons with SARS-CoV-2 infection using symptom monitoring and diagnostic testing (https://www.cdc.gov/coronavirus/2019-ncov/more/scientific-brief-options-to-reduce-quarantine.html). Accessed: 2020-12-16.

[32] Viner RM, et al. (2020) Susceptibility to SARS-CoV-2 infection among children and adolescents compared with adults: A systematic review and meta-analysis. *JAMA Pediatr.*

[33] Assaker R, et al. (2020) Presenting symptoms of COVID-19 in children: a meta-analysis of published studies. *Br. J. Anaesth.* 125(3):e330–e332.

[34] Rajmil L (2020) Role of children in the transmission of the COVID-19 pandemic: a rapid scoping review. *BMJ Paediatr Open* 4(1):e000722.

[35] Goldstein E, Lipsitch M, Cevik M (2020) On the effect of age on the transmission of SARS-CoV-2 in households, schools and the community. *J. Infect. Dis.*

[36] Stein-Zamir C, et al. (2020) A large COVID-19 outbreak in a high school 10 days after schools' reopening, israel, may 2020. *Eurosurveillance* 25(29):2001352.

[37] Ismail SA, Saliba V, Bernal JL, Ramsay ME, Ladhani SN (2020) SARS-CoV-2 infection and transmission in educational settings: a prospective, cross-sectional analysis of infection clusters and outbreaks in england.

[38] (2020) Covid-19 school response dashboard. Accessed: 2020-12-11.

[39] CDC (2020) Communities, schools, workplaces, & events (https://www.cdc.gov/coronavirus/2019-ncov/community/schools-childcare/index.html). Accessed: 2020-12-11.

[40] Larremore DB, et al. (2020) Test sensitivity is secondary to frequency and turnaround time for COVID-19 screening. *Sci Adv*.

[41] Denny TN, et al. (2020) Implementation of a pooled surveillance testing program for asymptomatic SARS-CoV-2 infections on a college campus - duke university, durham, north carolina, august 2-october 11, 2020. *MMWR Morb. Mortal. Wkly. Rep.* 69(46):1743–1747.

[42] Bergstrom T, Bergstrom CT, Li H (2020) Frequency and accuracy of proactive testing for COVID-19.

[43] (2020) Return to on-site sars-cov-2 testing protocols. *Color - Impact of proactive testing (2020)*.

[44] Karin O, et al. Cyclic exit strategies to suppress COVID-19 and allow economic activity.

[45] Zimmerman KO, et al. (2021) Incidence and secondary transmission of SARS-CoV-2 infections in schools. *Pediatrics*.

[46] Kampe EOi, Lehfeld AS, Buda S, Buchholz U, Haas W (2020) Surveillance of COVID-19 school outbreaks, germany, march to august 2020. *Eurosurveillance* 25(38):2001645.

[47] Polack FP, et al. (2020) Safety and efficacy of the BNT162b2 mRNA covid-19 vaccine. *N. Engl. J. Med.* 383(27):2603–2615.

[48] Baden LR, et al. (2020) Efficacy and safety of the mRNA-1273 SARS-CoV-2 vaccine. *N. Engl. J. Med.*

[49] Dooling K, et al. (2020) The advisory committee on immunization practices' interim recommendation for allocating initial supplies of COVID-19 vaccine - united states, 2020. *MMWR Morb. Mortal. Wkly. Rep.* 69(49):1857–1859.

[50] (2020) Teachers should be prioritized for vaccination against COVID-19 (https://www.unicef.org/press-releases/teachers-should-be-prioritized-vaccination-against-covid-19). Accessed: 2021-1-18.

[51] Korber B, et al. (2020) Tracking changes in SARS-CoV-2 spike: Evidence that D614G increases infectivity of the COVID-19 virus. *Cell* 182(4):812–827.e19.

[52] Leung K, Shum MH, Leung GM, Lam TT, Wu JT (2021) Early transmissibility assessment of the N501Y mutant strains of SARS-CoV-2 in the united kingdom, october to november 2020. *Euro Surveill.* 26(1).

[53] Rt.live (covid-19) (https://rt.live/). Accessed: 2021-1-17.

[54] Ismail SA, Saliba V, Bernal JL, Ramsay ME, Ladhani S (2020) SARS-CoV-2 infection and transmission in educational settings: Cross-Sectional analysis of clusters and outbreaks in england.

[55] Heavey L, Casey G, Kelly C, Kelly D, McDarby G (2020) No evidence of secondary transmission of COVID-19 from children attending school in ireland, 2020. *Euro Surveill.* 25(21).

[56] Macartney K, et al. (2020) Transmission of SARS-CoV-2 in australian educational settings: a prospective cohort study. *Lancet Child Adolesc Health* 4(11):807–816.

[57] Panovska-Griffiths J, et al. (2020) Determining the optimal strategy for reopening schools, the impact of test and trace interventions, and the risk of occurrence of a second COVID-19 epidemic wave in the UK: a modelling study. *Lancet Child Adolesc Health* 4(11):817–827.

[58] CDC (2020) Operating schools during COVID-19: CDC's considerations (https://www.cdc.gov/coronavirus/2019-ncov/community/schools-childcare/schools.html). Accessed: 2021-1-7.

[59] Gillespie DL ea (2021) The experience of two independent schools with in-person learning during the covid-19 pandemic. *In press, Journal of School Health*.

[60] Carsetti R, et al. (2020) The immune system of children: the key to understanding SARS-CoV-2 susceptibility? *Lancet Child Adolesc Health* 4(6):414–416.

[61] Bunyavanich S, Do A, Vicencio A (2020) Nasal gene expression of Angiotensin-Converting enzyme 2 in children and adults. *JAMA* 323(23):2427–2429.

[62] Leeb RT, et al. (2020) COVID-19 trends among School-Aged children - united states, march 1-september 19, 2020. *MMWR Morb. Mortal. Wkly. Rep.* 69(39):1410–1415.

[63] Brandal LT, et al. (2021) Minimal transmission of SARS-CoV-2 from paediatric COVID-19 cases in primary schools, norway, august to november 2020. *Euro Surveill.* 26(1).

[64] Fagnan J, Abnar A, Rabbany R, Zaiane OR (2018) Modular Networks for Validating Community Detection Algorithms. *arXiv:1801.01229 [physics]*. arXiv: 1801.01229.

[65] Newman MEJ, Park J (2003) Why social networks are different from other types of networks. *Physical Review E* 68(3).

[66] Read JM, Eames KT, Edmunds WJ (2008) Dynamic social networks and the implications for the spread of infectious disease. *Journal of The Royal Society Interface* 5(26):1001–1007.

[67] Salathe M, et al. (2010) A high-resolution human contact network for infectious disease transmission. *Proceedings of the National Academy of Sciences* 107(51):22020–22025.

[68] Barclay VC, et al. (2014) Positive Network Assortativity of Influenza Vaccination at a High School: Implications for Outbreak Risk and Herd Immunity. *PLoS One* 9(2).

[69] Levine-Tiefenbrun M, et al. (2020) Association of covid-19 rt-qpcr test false-negative rate with patient age, sex and time since diagnosis. *medRxiv*.

[70] CDC (2020) Duration of isolation and precautions for adults with COVID-19 (https://www.cdc.gov/coronavirus/2019-ncov/hcp/duration-isolation.html). Accessed: 2020-12-16.

Appendix A Model Description

Contents

A.1 SEIRS+ Extended SEIR Network Model . . . 31
A.1.1 Heterogeneity . . . 32
A.1.2 Compartments . . . 32
A.1.3 Dynamics . . . 33
A.1.4 Transmission . . . 34
A.1.4.1 Global transmission . . . 35
A.1.4.2 Local transmission . . . 35
A.2 School Models . . . 36
A.2.1 Disease progression parameters . . . 36
A.2.2 Transmission parameters . . . 37
A.2.3 Contact Networks . . . 41
A.2.3.1 Primary school contact networks . . . 41
A.2.3.2 Secondary school contact networks . . . 41
A.2.3.3 Quarantine contact networks . . . 42
A.2.3.4 Weekend contact networks . . . 42
A.2.3.5 Cohort contact networks . . . 42
A.2.4 Case Introductions . . . 47
A.2.5 Interventions . . . 48
A.2.5.1 Simulation loop . . . 48
A.2.5.2 Testing . . . 49
A.2.5.3 Cohorting . . . 50
A.2.5.4 Isolation . . . 51
A.2.5.5 Vaccination . . . 52

A.1 SEIRS+ Extended SEIR Network Model

SEIRS+ is an open source Python framework developed by McGee et al. that supports flexible parameterization and implementation of sophisticated epidemiological models (https://github.com/ryansmcgee/seirsplus). The models studied in this work are parameterizations of the stochastic Extended SEIR Network Model provided in the SEIRS+ framework. We simulate our models using the Interventions Simulation Loop provided in SEIRS+ with minor modifications for our particular school context. Extensive documentation for the models, simulation loops, and other features of SEIRS+ can be found on the SEIRS+ github wiki (https://github.com/ryansmcgee/seirsplus/wiki).

A.1.1 Heterogeneity

In the SEIRS+ Extended SEIR Network Model, individuals are represented as nodes in a contact network, and all parameters, interactions, and interventions can be specified on a node-by-node basis. Therefore, this model enables explicit representation of heterogeneity in disease characteristics, contact patterns, and behaviors, which are important for modeling small, age-stratified populations such as schools. Parameter choices and distributions for our school models are described in the School Models appendix section.

A.1.2 Compartments

The Extended SEIR Network Model extends the classic SEIR model of infectious disease to represent pre-symptomatic, asymptomatic, and symptomatic disease states, which are of particular relevance to the SARS-CoV-2 pandemic. The classic SEIR model divides the population into susceptible (S), exposed (E), infectious (I), and recovered (R) individuals. In this extended model, the infectious subpopulation is further subdivided into pre-symptomatic (I_{pre}), asymptomatic (I_{asym}), and symptomatic (I_{sym}) compartments, all of which represent contagious individuals (the full Extended SEIR Network Model includes a hospitalized infectious state, but we assume no hospitalization in this report and effectively ignore this compartment). Individuals transition from one compartment to the next at times determined by the disease characteristics (see Appendix A.2.1 Disease progression parameters). A parameterizable fraction of the population are deemed asymptomatic and will progress to the asymptomatic compartment when exiting the presymptomatic compartment, while the remainder of the population will progress to the symptomatic compartment. The dynamics of compartment transitions are described further in the Dynamics appendix section.

The effect of isolating individuals in response to symptoms or testing is modeled by introducing compartments that represent quarantined individuals (Figure Figure A1). An individual may be quarantined in any disease state, and every disease state has a corresponding quarantine compartment. Quarantined individuals follow the same progression through the disease states, but their set of close contacts are defined by a distinct quarantine contact network (Appendix A.2.3 Contact Networks). In this work, individuals are moved into quarantine states by the Intervention Simulation Loop (Appendix A.2.5.1), such as when a positive test result is returned, as opposed to according to a transition rate. Individuals remain in the quarantine compartment flow until the designated isolation period has been reached (10 days in this work), at which time they are moved into the non-quarantine compartment corresponding to their current disease state.

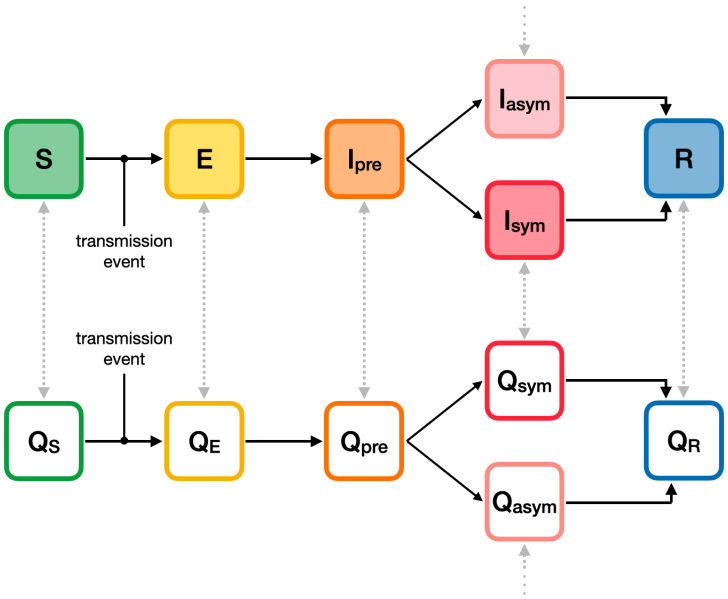

Figure A1: Compartment model. The compartment model that defines the progression of disease states in the Extended SEIR Network Model.

A.1.3 Dynamics

Transmission dynamics are simulated using the Gillespie algorithm, a common and rigorous method for simulating stochastic interaction dynamics. Briefly, the system's differential equations are adapted to compute the 'propensity' of the possible events (i.e., the expected amount of time until a given event will take place) for all nodes at each time step. These propensities are then used to compute the probabilities of all possible state events normalized across the entire population. A random node and corresponding transition are selected to execute according to these probabilities in each time step. The propensities of transmission events (S to E transitions) are proportional to the product of the prevalence of infectious individuals among each node's contacts and the transmissibilities and susceptibilities of the interacting individuals (see Appendix A.1.4 Transmission).

SEIRS+ supports calculating the propensities of disease progression transitions (e.g., E to I_{pre}, Q_{pre} to Q_{sym}) in two different ways: 1) using transition rates (standard Gillespie implementation), or 2) using compartment residence times. Running the model in the first mode results in exponentially distributed residence times in each compartment, as in classic mass action SEIR-like models. In the latter mode, each individual is assigned a residence time for each compartment, and the propensity for a given individual to transition out of the current state is 0 until this residence period has elapsed, at which time this propensity becomes large such that the next event will be this given individual transitioning to the next compartment with probability approaching 1. This results in a hybrid model where transmission events occur stochastically according to the Gillespie algorithm while other disease progression transitions occur in a clock-like manner in parallel. In reality, res-

idence times in disease states are not well-described by exponential distributions. As such, we use the residence time propensity calculation mode in this work and assign heterogeneous residence times to individuals drawn from gamma distributions that better match empirical descriptions of the disease dynamics for COVID-19 (Appendix A.2.1).

For more information about the propensity equations, refer to https://github.com/ryansmcgee/seirsplus/wiki.

A.1.4 Transmission

The dynamics governing transmission events that cause susceptible individuals to become exposed are arguably the most important to understand in any epidemiological model, so we break down the transmission dynamics of the Extended SEIR Network Model in detail here.

In general, the propensity $P^{(i)}(S \to E)$ of a given susceptible individual i becoming infected is proportional to the product of the prevalence of infectious individuals among their contacts, the average transmissibility of their infectious contacts $\overline{\beta}^{(\text{contacts})}$, and their own susceptibility to infection $\alpha^{(i)}$.

$$P^{(i)}(S \to E) \propto \alpha^{(i)} \times \overline{\beta}^{(\text{contacts})} \times (\text{prevalence among contacts})$$

An individual's transmissibility $\beta^{(i)}$ (i.e., transmission rate) is equal to the expected number of cases that this individual would generate in a fully-susceptible population (i.e., the reproduction number for the individual, $R_0^{(i)}$ divided by the length of their infectious period $\gamma^{(i)}$.

$$\beta^{(i)} = \frac{R_0^{(i)}}{\gamma^{(i)}}$$

For the purposes of the models considered in this work, the propensity of a given individual i becoming infected is calculated using the following equation[1], which we will break down in the rest of this section

$$P^{(i)}(S \to E) = \alpha^{(i)} \left[p \underbrace{\left(\frac{\bar{\beta}\left(I_{\text{pre}} + I_{\text{sym}} + I_{\text{asym}}\right)}{N} \right)}_{\text{global transmission}} + (1-p) \underbrace{\left(\frac{\sum_{j \in C_G^{(i)}} \delta^{(ji)} \left(\beta^{(ji)} \mathbf{1}_{X^{(j)} \in \{I_{\text{pre}}, I_{\text{sym}}, I_{\text{asym}}\}} \right)}{|C_G^{(i)}|} \right)}_{\text{local transmission}} \right]$$

In this model, disease transmission may occur either from close contacts defined by the contact network structure or from casual contacts. Close contacts are individuals with whom one has repeated, sustained, or close proximity interactions on a regular basis: classmates, friends, housemates, or other close relationships. In contrast, casual contacts are individuals with whom one has

[1] This equation is simplified from the general equation implemented in the Extended SEIR Network Model, which includes parameters and terms that are not used here and are thus zeroed out.

incidental, brief, or superficial contact on an infrequent basis and to whom one is not connected directly on the network. A network locality parameter p sets the relative frequency and weight of transmission among close (local network) and casual (global) contacts in the model population.

A.1.4.1 Global transmission A fraction p of a given individual's interactions are with casual contacts, which are assumed to be individuals randomly sampled from the population at large, irrespective of the contact network. With respect to these global interactions, every node in the population is equally likely to come into contact with every other node, and the population can be considered well-mixed. Thus the propensity of global transmission is calculated in the same way as mass action compartment models that assume a well-mixed population. The propensity for a given susceptible individual to become exposed due to global transmission is proportional to the product of that individual's susceptibility $\alpha^{(i)}$, the population mean transmissibility of infectious individuals $\overline{\beta}$, and the prevalence of infectious individuals in the overall population $(I_{\text{pre}} + I_{\text{sym}} + I_{\text{asym}})/N$.

A.1.4.2 Local transmission A fraction $1 - p$ of a given individual's interactions are with individuals from their set of "close contacts." An individual's close contacts are defined as the nodes adjacent to the given node in the contact network ($C_G^{(i)}$ denotes the set of close contacts for individual i: the nodes adjacent to node i in the contact network graph G). With respect to local transmission, transmissibility is considered on a pairwise basis. That is, every directed edge of the contact network representing transmission from infected node j to susceptible node i is assigned a transmissibility weight $\beta^{(ji)}$. The transmissibility of such an interaction is assumed to be equal to the transmissibility of the infected individual (i.e., $\beta^{(ji)} = \beta^{(j)}$). The propensity for a given susceptible individual to become exposed due to local transmission is calculated as the product of that individual's susceptibility and the sum transmissibility of their infectious close contacts ($\mathbf{1}_{X^{(j)} \in \{I_{\text{pre}}, I_{\text{sym}}, I_{\text{asym}}\}}$ is an indicator function that takes the value 1 when the state $X^{(j)}$ of the contact node j is one of the infectious states and 0 otherwise), divided by the size of their local network ($|C_G^{(i)}|$ denotes the size of the set of close contacts for individual i).

This amounts to the propensity of exposure for node i being proportional to the product of their susceptibility and the transmissibility-weighted prevalence of infectious individuals in their local network. Thus, propensity for exposure due to local transmission is frequency dependent and analogous to the propensity contribution from global transmission. Implicit in this formulation is an assumption that all individuals have an equal interaction budget (e.g., equal amount of time or intensity interacting with others), and individuals with more close contacts (i.e., higher degree) interact less with each contact and are therefore less likely to become exposed by any single individual. An additional factor $\delta^{(ji)}$ appears in the calculation of propensity for exposure due to

local transmission. This pairwise factor is used to re-weight the transmissibility of interactions according to the connectivity of the interacting individuals. Here we are interested in re-weighting in order to counteract, in part, the aforementioned implicit assumption that all individuals have an equal interaction budget. While it is reasonable to think that individuals (e.g., secondary school teachers) who have many contacts (e.g., students) do not interact as closely with each of their contacts as another individual who only has a handful of contacts, we do not assume that the propensity of infection decreases linearly with degree for SARS-CoV-2 transmission. We define the degree scaling factor $\delta^{(ji)}$ as

$$\delta^{(ji)} = \frac{\log(D^{(i)}) + \log(D^{(j)})}{2\log(\overline{D})}$$

where $D^{(j)}$ and $D^{(i)}$ are the degrees of nodes j and i, respectively, and $\overline{D}$ is the mean degree of the network. Using this definition of $\delta^{(ji)}$, when two individuals whose average degree is an order of magnitude greater than the average degree of the population overall, then the propensity of exposure in their interaction is twice that of two averagely-connected individuals. Thus, the propensity for infection by a single infectious contact is lower for highly-connected individuals compared to low connectivity individuals, but not proportionally so.

A.2 School Models

The following sections describe the specific assumptions and parameter values used to define the primary and secondary school models studied in this work. These models were implemented using the SEIRS+ framework's Extended SEIR Network Model (see Appendix A.1 SEIRS+ Extended SEIR Network Model).

A.2.1 Disease progression parameters

As described in Appendix A.1.3 Dynamics, individuals remain in each compartment (excluding Susceptible) for a designated period of time before progressing to the next disease state. The population is heterogeneous for each disease state period, with each individual being assigned disease state periods drawn from gamma distributions that are informed by empirical studies of COVID-19 progression. Refer to Table A.2.1 for more information about each distribution. We assume that the distributions of disease state periods are the same for all age groups and for both quarantined and non-quarantined individuals. The same gamma distribution parameters are used to define the period probability distributions in every simulation, but the period values are randomly drawn and assigned in each replicate.

Additionally, we assume that 30% of adults and secondary school students are asymptomatic, and that 40% of primary school students (young children) are asymptomatic. In the initialization of each simulation, each individual in the population is randomly assigned a symptomatic or

asymptomatic status according to these probabilities. If an individual becomes infected, they will progress to the symptomatic (I_{sym}) or asymptomatic (I_{asym}) state when exiting the pre-symptomatic (I_{pre}) state according to this assigned status. 20% of symptomatic individuals self-isolate upon entering the symptomatic state, but there are no other parameter differences between symptomatic and asymptomatic individuals in our model.

A.2.2 Transmission parameters

As described in Appendix A.1.4 Transmission, the propensity of transmission events depend on the transmissibility and susceptibility parameters of interacting individuals. Each individual is assigned an individual reproduction number $R_0^{(i)}$, which is the expected number of secondary cases that the individual generates when infectious in a fully susceptible pouplation. Each individual reproduction number is converted to an individual transmissibility (i.e., transmission rate) parameter using the following standard formula

$$\beta^{(i)} = \frac{R_0^{(i)}}{\gamma^{(i)}} ,$$

where $\gamma^{(i)}$ is the total infectious period for individual i. We assume that individual transmissibility is heterogeneous and follows an overdispersed (long-tailed) distribution that corresponds approximately to 20% of individuals contributing 80% of the total expected number of secondary cases (the 80/20 rule). We calibrate the individual reproduction number distribution such that its mean corresponds to a chosen average basic reproduction number R_0 for the population (R_0=1.5 and R_0=2.25 are considered in the main text) and so that 80% of the weight falls in the upper 20th percentile of individuals in the tail of the distribution. Therefore, for any R_0 considered in this paper, many individuals are expected to generate fewer than 1 secondary case while a minority of individuals are expected to contribute a large number. Refer to Table A.2.2 for more information about these distributions. We assume that all age groups have transmissibilities drawn from the same distribution. In addition, we assume there is no difference in transmissibility between the pre-symptomatic, symptomatic, and asymptomatic states (i.e., the same individual transmissibility is used while an individual is in any one of these states).

Additionally, individuals are assigned a susceptibility parameter value, which weights the propensity that they become infected by any infectious contacts they may have (see Appendix A.1.4 Transmission). Adults and secondary students are assigned the baseline susceptibility value of 1.0, and thus their propensity of infection is based on the unweighted transmissibilities of their contacts. In the main text, primary school students (young children) are assumed to be 60% as susceptible as adults. Therefore, primary school students are assigned a susceptibility value of 0.6, and their propensity of infection is only 60% of that of an adult in the same infectious contact context.

We assume that 80% of transmission is attributable to close contacts (local transmission on

the contact network) and 20% is attributable to casual contacts (i.e., global transmission among the overall population)(see Appendix A.1.4 Transmission). Global transmission can be thought to represent both casual interactions among members of the school population while on campus as well as relatively infrequent interactions among members of the school population while off campus (e.g., on weekends and off-cohort days).

Table A.2.1 A representative distribution of period values drawn for a secondary school with 1,000 individuals is shown for each parameter in the center column below. Statistics across all replicate distributions in our analysis are shown in the rightmost column.

Disease state period	**Distribution**	**Statistics**
Latent period (time in E state)	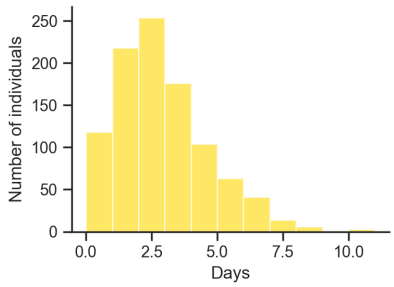 `gamma(mean=3.0, CV=0.6)`	mean 3.0 days std 1.8 days 95% CI (0.6, 7.4)
Pre-symptomatic period (time in I_{pre} state)	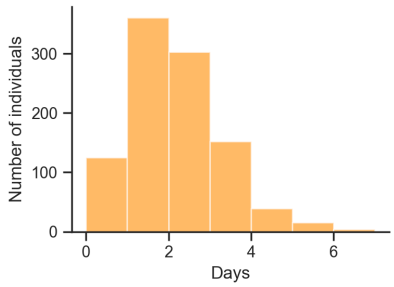 `gamma(mean=2.2, CV=0.5)`	mean 2.2 days std 1.1 days 95% CI (0.6, 4.8)
Symptomatic period (time in I_{sym} or I_{asym} state)	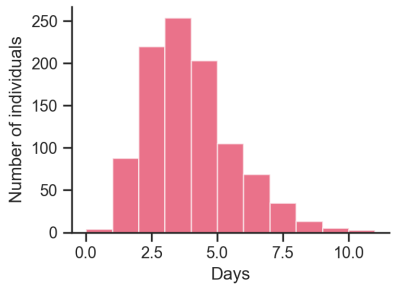 `gamma(mean=4.0, CV=0.4)`	mean 4.0 days std 1.6 days 95% CI (1.5, 7.6)
Total infectious period (total time in I_{pre}, I_{sym}, and I_{asym} states)	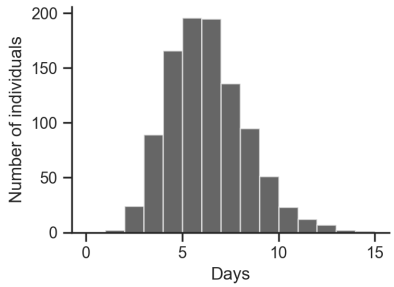 `gamma(mean=2.2, CV=0.5)`	mean 6.2 days std 1.9 days 95% CI (3.0, 10.5)

Table A.2.2 A representative distribution of drawn individual reproduction number values for a secondary school with 1,000 individuals is shown for the basic reproduction numbers considered in the main text below. Statistics across all replicate distributions in our analysis are shown in the rightmost column.

Population R_0	**Distribution of individual reproduction numbers $R_0^{(i)}$**	**Statistics**
R_0 = 1.5	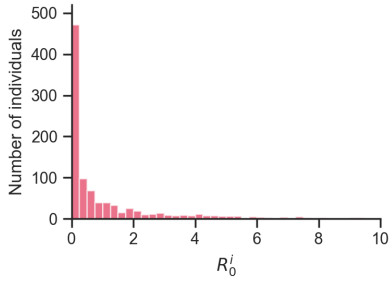 `gamma(mean=1.5, CV=2.0)`	mean 1.5 std 3.0 median 0.26 95% CI (0, 10.2) 80th percentile: 2.2 31% of values > 1.0
R_0 = 2.25	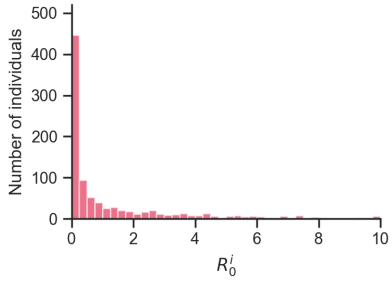 `gamma(mean=2.25, CV=2.0)`	mean 2.25 std 4.5 median 0.39 95% CI (0, 15.45) 80th percentile: 3.3 38% of values > 1.0

A.2.3 Contact Networks

The SEIRS+ Extended SEIR Network Model allows arbitrary graphs to be used to specify the contact network that defines close contacts for local transmission (see Appendix A.1.4 Transmission). Here we define distinct networks representing the contact structure of a primary school and a secondary school.

A.2.3.1 Primary school contact networks For our primary school model, we simulate a medium-sized school of 480 students with 24 teachers and 24 additional staff. Each class comprises one teacher and 20 students in mutual contact. That is, the students and teacher for each classroom are strongly connected. Additionally, each teacher interacts with a handful of other teachers and staff, and students that share the same household are connected (the percentage of primary school aged children that share a household with another primary school aged child is calibrated by US census data). Most of the contacts that an individual makes in the school population are with the students and teacher in their own class, and disease transmission within a class is more likely than between classes. The FARZ algorithm, which generates random networks with built-in community structure and broad, heavy-tailed degree distributions that are realistic for human contact networks (20, 21, 64–66). Refer to Table A.2.3a for more information about the parameterization of these networks, and see Table A.2.3b for more information about the their degree and other network properties.

A.2.3.2 Secondary school contact networks For our secondary school model, we consider a medium-sized school with 800 students (200 per graduating class), 125 teachers, and 75 staff. We generate network layers for students and teachers and staff using the FARZ network generation algorithm, which allows us to calibrate epidemiologically-important network properties (e.g., cluster structure, assortativity, and clustering coefficient) to values consistent with studies of secondary school contact networks (67, 68). A FARZ network layer is generated for each grade, with students belonging to one or more social groups (i.e., network clusters) of about 10 individuals each. 80% of each student's contacts are with students in the same grade, and 80% of those within-grade contacts are with students in their own social groups. Students that share a household are connected as well (the percentage of secondary school aged children that share a household with another secondary school aged child is calibrated by US census data). Interactions between teachers and staff are represented by another FARZ network layer. Finally, students are connected with six random teachers with whom they have classes. Each teacher is associated with a grade level, and students take classes with teachers in their own grade level 75% of the time, which leads to students in the same grade being more likely to share teachers. A unique random network is generated as described for each simulation replicate. Refer to Table A.2.3c for more information

about the parameterization of these networks, and see Table A.2.3d for more information about the their degree and other network properties.

A.2.3.3 Quarantine contact networks When individuals are in quarantine, a separate quarantine contact network is referenced when calculating propensities of transmission involving that individual. Here we define the contact network as the school contact network minus all edges except for connections between housemates. That is, a quarantined individual makes contact with their housemates (e.g., siblings) but no one else from the school population. Global transmission is set to 0 for individuals in quarantine as well.

A.2.3.4 Weekend contact networks The contact network that is in effect on weekends is the same as the quarantine network. That is, individuals only have direct contacts with housemates on weekends. However, global transmission is left at 20% for non-quarantined individuals on weekends to represent general mixing among the school population when out of school.

A.2.3.5 Cohort contact networks One of the mitigations we consider is student cohorting, in which students are divided into two groups, only one of which attends school on any given day (see Appendix A.2.5.3 Cohorting). In our model, cohorting is implemented by alternating between two modified school contact networks. Students are divided into two cohorts, A and B. Primary students are divided such that exactly half of each classroom is in each cohort. Secondary school students are arbitrarily divided (even and odd node indexes). A modified contact network is then generated to represent when cohort A is onsite, and one is generated to represent when cohort B is onsite. Each cohort network removes all edges from offsite students, except for their household connections, while maintaining the edges of onsite students. These networks are alternated according to the given cohorting schedule, when applicable.

The degree-based pairwise transmissibility factors $\delta^{(ji)}$ (See Appendix A.1.4.2 Local transmission for details) are calculated according the the connectivities of individuals in the baseline, "everyone onsite" network. The same set of factors derived from this baseline are used to calculate the propensities of local transmission at all times (i.e., for all school days, weekend days, and cohorting days), regardless of which cohort or weekend network is being used to define the structure of close contacts. This reflects an assumption that, for example, the interactions between individuals who are on campus don't become more intense under cohorting just because fewer students are on campus.

Table A.2.3a Parameters for the generation of primary school contact networks.

Parameter	Value	Additional description
Number of grades	6 (K-5)	
Number of classes per grade	4	
Number of students per class	20	
Number of teachergroups	1	FARZ parameter for teacher/staff layers: Number of network clusters in teacher/staff layer
Teacher/staff mean degree	5	Average number of connections each teacher/staff makes with other teachers/staff
`alpha`	5	FARZ parameter for teacher/staff layers: Strength of common neighbor's effect on edge formation (tunes transitivity, clustering)
`gamma`	5	FARZ parameter for teacher/staff layers: Strength of degree similarity effect on edge formation (tunes assortativity)

Table A.2.3b Degree distribution plots for a representative primary school network and network property statistics averaged across all primary school contact networks used in our analysis.

Network	**Degree distribution**	**Network properties**
Overall network	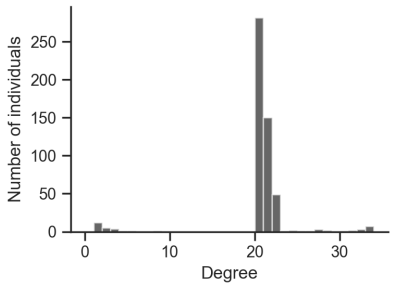	Degree mean: 20.1 Degree std: 4.5 Degree CV^2: = 0.5 Degree assortativity: 0.20 Clustering coeff.: 0.91 Average path length: 3.6
Student-Student layer	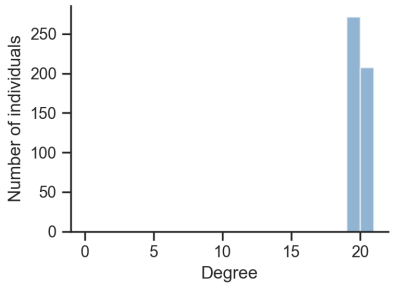	Degree mean: 19.5 Degree std 0.6 Degree CV^2 = 0.0 Degree assortativity: 0.05 Clustering coeff.: 0.95 Average path length: 3.9
Teacher-Staff layer	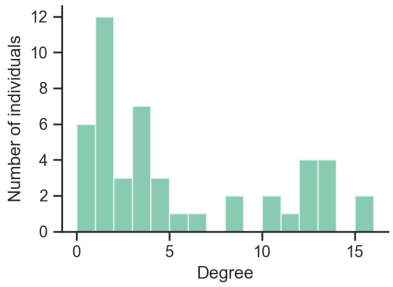	Degree mean 5.0 Degree std 4.8 Degree CV^2 = 0.8 Degree assortativity: 0.46 Clustering coeff.: 0.49 Average path length: 3.6

Table A.2.3c Parameters for the generation of secondary school contact networks.

Parameter	Value	Additional description
Number of grades	4	
Number of students per grade	200	
Number of teachers	125	
Number of staff	75	
Number of classes per student	6	Number of classes that each student takes each day; i.e., number of teachers with whom each student is connected
Percentage of student-teacher grade level matches	75%	Probability that a student takes a class with, i.e., connects to, a teacher that is associated with their own grade level
Number of student social groups per grade	20	FARZ parameter for student layers: Number of network clusters in each student layer
Student mean intra-grade degree	16	Average number of connections each student makes with students in the same grade
Student percent inter-grade contacts	20%	Percent of each student's total student connections that are with students in another grade
Number of teacher/staff groups	10	FARZ parameter for teacher/staff layers: Number of network clusters
Teacher/staff mean degree	10	Average number of connections each teacher/staff makes with other teachers/staff
`alpha`	5	FARZ parameter for all layers: Strength of common neighbor's effect on edge formation (tunes transitivity, clustering)
`gamma`	5	FARZ parameter for all layers: Strength of degree similarity effect on edge formation (tunes assortativity)
`beta`	0.8	FARZ parameter for all layers: Probability of edges formation within clusters (strength of cluster structure)
`r`	2	FARZ parameter for all layers: Maximum number of clusters each node can belong to
`q`	0.5	FARZ parameter for all layers: Probability of a node belonging to the multiple clusters

Table A.2.3d Degree distribution plots for a representative secondary school network and network property statistics averaged across all primary school contact networks used in our analysis.

Network	Degree distribution	Network properties
Overall network	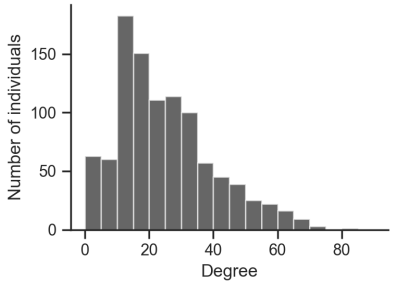	Degree mean: 24.1 Degree std: 15.0 Degree CV^2: = 0.39 Degree assortativity: -0.10 Clustering coeff.: 0.16 Average path length: 2.6
Student-Student layer	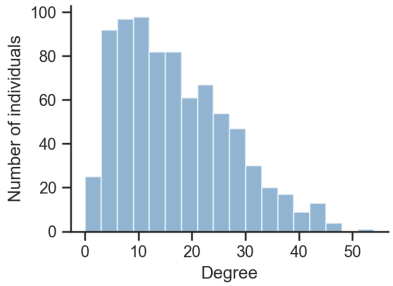	Degree mean: 16.0 Degree std 10.1 Degree CV^2 = 0.39 Degree assortativity: 0.16 Clustering coeff.: 0.22 Average path length: 2.9
Teacher-Staff layer	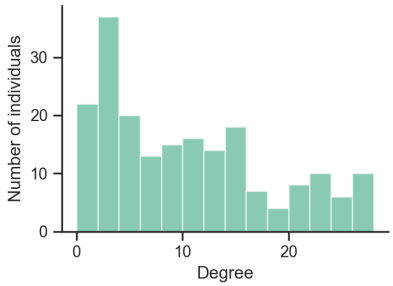	Degree mean 10.0 Degree std 8.2 Degree CV^2 = 0.64 Degree assortativity: 0.39 Clustering coeff.: 0.40 Average path length: 2.7

A.2.4 Case Introductions

Exposure to the community is modeled by randomly introducing new cases to the school population according to a Poisson process with an average introduction rate that corresponds to the community prevalence. Each day of the simulation, the number of introductions is drawn from a Poisson distribution using the given introduction rate as the Poisson parameter λ. Then for each exposure that is to be introduced (if greater than zero), an individual is drawn randomly from the population with selection probabilities proportional to the relative susceptibility of each individual. If the selected individual(s) are susceptible, they become exposed (infected)—otherwise they have been previously infected and their state is left unchanged. This process is handled within the simulation loop adapted from the SEIRS+ Intervention Simulation Loop (Appendix A.2.5.1).

We consider monthly, weekly, and daily introduction rates, as well as single introduction scenarios. These rates roughly correspond to the community prevalences shown in Table 1. These associations between the community prevalence and the rate of introduction to the school population are approximated using the following method. The expected number of new cases to be generated in the overall community is approximated using the equation for the change in the number of infected individuals from the classic SIR model

$$dI_c = \frac{\beta_c S_c I_c}{N_c} = \beta_c S_c \pi_c \,,$$

where dI_c gives the expected number of new infections in the community per day, N_c is the size of the community, β_c is the average community transmission rate, S_c is the number of susceptible individuals in the community, and $\pi_c = I_c/N_c$ is the community prevalence (the subscript c denotes a community value). Then the number of these new cases that will land in the school population is assumed to be proportional to the ratio of the size of the school population to the overall community population.

$$\text{expected school introduction rate} = \frac{\beta_c S_c I_c}{N_c} \frac{N}{N_c} \,.$$

When the numbers of current and prior cases in the community (I_c and R_c, respectively) are small relative to the size of the community (i.e., $S_c \approx N_c$; this estimation will tend to overestimate the school introduction rate when there is significant susceptible depletion in the community), this can be simplified to a reasonable approximation that does not depend on the size of the overall

community

$$
\begin{aligned}
\text{expected school introduction rate} &= \frac{\beta_c S_c I_c}{N_c} \frac{N}{N_c} \\
&= \frac{\beta_c (N_c - I_c - R_c) I_c}{N_c} \frac{N}{N_c} \\
&\approx \frac{\beta_c N_c I_c}{N_c} \frac{N}{N_c} \\
&= \frac{\beta_c I_c}{N_c} N \\
&= \beta_c \pi_c N \,.
\end{aligned}
$$

Thus the expected rate of introductions to the school population approximately equal to the product of the community transmission rate β_c, the community prevalence π_c, and the size of the school population N. The community transmission rate is equal to the effective reproduction number R_{eff} for the community divided by the average infectious period of the disease. Given estimates for these values, the introduction rate can be estimated. This method was used to estimate introduction rates for primary schools (N=528) and secondary schools (N=1,000) for R_{eff} in the range (1.0, 2.0), a mean infectious period of 6.5 days, and a range of community prevalence values. The community prevalence ranges for each introduction rate listed in Table 1 are those prevalences for which the expected number of new cases per day in the school population is approximately equal to the listed introduction rate (monthly, weekly, or daily) for some Reff in (1.0, 2.0) using this method and these parameters.

A.2.5 Interventions

We model several interventions for mitigating the spread of SARS-CoV-2. The SEIRS+ framework provides code for a simulation loop that can implement several interventions, including testing, tracing, and isolation. We make use of a subset of the features in this simulation loop (with minor modification) to implement the mitigation strategies studied in this work.

A.2.5.1 Simulation loop

The simulation loop repeatedly calls a function that iterates the Gillespie dynamics of the Extended SEIR Network Model, which determines the next compartment transition (transmission event or disease progression) that will take place, advances the simulation time to the time of that event, and executes the state update. Every time the simulation time crosses an integer value (i.e., a new day is reached), the simulation loop interfaces with the model and its nodes, states, and parameters to implement various intervention procedures. If the Gillespie time to the next event is greater than a day, the simulation advances by a maximum time step that is a fraction of a day to ensure that

intervention days are not skipped or irregularly timed. The simulation loop performs the following updates each iteration:

1. Advance the Gillespie compartment transition dynamics
2. If a new day has been reached, execute the following; else Return to (1):
   (a) Update active contact networks and parameters according to the weekend and cohorting schedule when applicable (see Appendix A.2.5.3 Cohorting and Appendix A.2.3.5 Cohort contact networks).
   (b) Introduce new community exposure cases (see Appendix A.2.4 Case Introductions).
   (c) Isolate symptomatic individuals who are compliant with self-isolation upon symptom onset (see Appendix A.2.5.4 Isolation).
   (d) If the current day is part of the testing cadence, test individuals who are eligible for testing when applicable (see Appendix A.2.5.2 Testing); else skip.
   (e) Isolate individuals who have received a positive test result (following the test result lag time) and in some cases their classmates when applicable (see Appendix A.2.5.4 Isolation)
   (f) Return to (1)

More details about these interventions are provided in the following sections.

A.2.5.2 Testing

We consider proactive testing that is executed according to one of several testing cadences (including no testing) shown in Table 2. These cadences define which groups of individuals are tested and on which days of the week. On a designated testing day, all individuals who are eligible to be in the testing pool are tested. An individual is considered part of the testing pool when they:

- Are a member of one of the groups designated in the testing cadence
- Are not currently in isolation
- Have not already had a positive test result
- Have not already recovered from the disease
- Have not been vaccinated
- Are compliant with testing

We assume that 100% of teachers and staff are compliant with testing, but 25% of students are non-compliant and thus never get tested. Students are assigned a compliance status randomly according to this probability when the model is initialized.

We model realistic temporal test sensitivities consistent with PCR tests. We assume 0% sensitivity for individuals in the exposed (latent) state. We assume 75% sensitivity for individuals in the first 2 days of their pre-symptomatic period and 80% sensitivity for any pre-symptomatic days beyond that. Sensitivities for symptomatic and asymptomatic individuals alike follow the time course shown in Figure A2, which follows from Levine-Tiefenbrun et al (69). We assume there are no false positives.

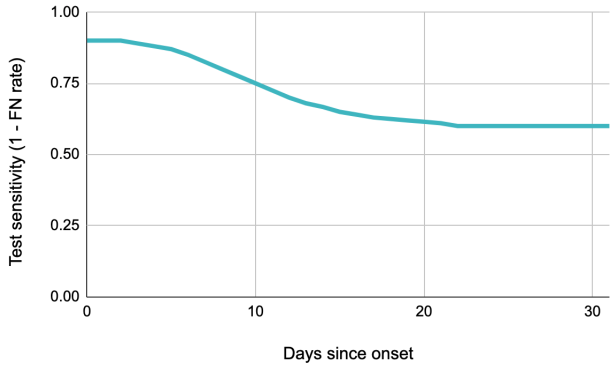

Figure A2: Test sensitivities. The probability of returning a positive test results when testing an individual in a symptomatic (I_{sym} or asymptomatic I_{asym} infectious state as a function of the number of days since entering that state (i.e., days since onset of symptoms). The test sensitivity is equivalent to 1 minus the false negative rate.

There is a 1 day lag (exactly 24 hours) between administering a test and receiving the result. Individuals that receive a positive result enter isolation (i.e., move into a quarantine compartment) immediately upon receiving the positive result, thus 1 day after being tested. We assume that all individuals in the school population are compliant with entering isolation upon a positive test result.

A.2.5.3 Cohorting

Cohorting consists of dividing students into two groups and following an alternating schedule in which only one group is on campus at a time. We consider two cohorting schedules, one where the group of students that is onsite alternates daily, and one where the onsite group alternates weekly (in addition to no cohorting). The cohorting schedules are summarized in Figure A3.

Cohorting is implemented by alternating between different versions of the contact network in which one group of students or the other has their connections with the school population removed, except for any connections to individuals in their own household. Global transmission remains active for students who are offsite due to the cohort schedule, which can be thought of as students having some propensity to interact with other members of the school population outside of school. We assume that all students comply with the cohorting schedule. Students who are offsite due to

Cohort Schedule		Mon	Tue	Wed	Thu	Fri	Sat	Sun
All Students Onsite	Week 1	AB	AB	AB	AB	AB		
	Week 2	AB	AB	AB	AB	AB		
Alternate A/B Cohorts Daily	Week 1	A	B	A	B	A		
	Week 2	B	A	B	A	B		
Alternate A/B Cohorts Weekly	Week 1	A	A	A	A	A		
	Week 2	B	B	B	B	B		

A Cohort A on campus B Cohort B on campus

Figure A3

cohorting are not considered to be in isolation, and these students are still part of the testing pool when otherwise applicable.

A.2.5.4 Isolation

When an individual enters isolation, they are moved into the quarantine compartment that corresponds to their disease state at the time of isolation. This compartment transition is executed "manually" by the simulation loop, separate from the Gillespie or residence time-based transition dynamics (Appendix A.1.3 Dynamics). While in isolation, individuals transition between quarantine compartments according to the same disease state residence times that are used when not in isolation. The set of close contacts for isolated individuals is given by a distinct quarantine contact network, which includes connections to members of the quarantined individual's household but no other members of the school population. In addition, quarantined individuals make no casual contacts (i.e., no global transmission). Isolated individuals remain in the quarantine sequence of compartments until their total isolation period has elapsed, at which time they are moved into the non-quarantine compartment that corresponds to their current disease state. We use a 10 day isolation period for all individuals, following the current CDC recommendation (70).

In this model, individuals may enter isolation upon the onset of symptoms (if compliant), after receiving a positive test result, or when another member of their classroom has tested positive (for primary schools, when applicable).

We assume that 20% of all individuals elect to self-isolate upon the onset of symptoms. The symptomatic isolation compliance status of individuals is assigned randomly according to this probability when the model is initialized. For compliant individuals, there is a 1 day lag between transitioning into the symptomatic compartment and entering isolation. Individuals who are asymptomatic and thus enter the asymptomatic compartment rather than the symptomatic compartment never self-isolate. Note that the rate of asymptomatic disease is assumed to be different in primary school-aged children (40%) and adults/adolescents (30%) while the rate of symptomatic isolation compliance is constant, so the effective rate of symptomatic self-isolation is lower in

young children.

In primary schools, where classroom groupings are stable, we also consider scenarios where entire classrooms (i.e., all students and the teacher) isolate when any one member of the classroom tests positive. In such a case, the entire group enters isolation at the same time immediately after the index case receives their test result (i.e., 1 day after being tested).

A.2.5.5 Vaccination

We also evaluate the effectiveness of vaccinating teachers and staff on mitigating transmission in schools. We use the following working definitions with regard to vaccination in this model:

- Uptake: The percentage of individuals who receive a vaccine
- Effectiveness: The percentage of individuals receiving the vaccine that have an efficacious response. An efficacious response is characterized by an immune response that protects the vaccinated individual from falling ill and that reduces the individual's transmissibility to some extent.
- Reduction in transmissibility: The factor by which individual transmissibility is reduced for individuals with an efficacious response to vaccination

We model the scenario where 100% of teachers and staff are vaccinated with a vaccine that has 90% effectiveness (and no students are vaccinated), and we consider scenarios where an effective vaccine blocks 100% of transmission (i.e., the vaccinated individual's transmissibility is reduced to 0) and where it only blocks 50% of transmission (i.e., the vaccinated individual's transmissibility is reduced to 50% its original value). The individuals that are to have an effective response are chosen randomly according to the probability of effectiveness when the model is initialized. Teachers are vaccinated and individuals with effective responses have their transmissibilities reduced before the simulation time begins. Individuals with effective immune responses are not included in case counts due to their immunity to the disease. Individuals with ineffective responses have no change in transmissibility or other parameters, can still contract and transmit the virus, and are included in case counts.